bioRxiv preprint doi: https://doi.org/10.1101/2020.02.13.948091; this version posted February 13, 2020. The copyright holder for this preprint (which was not certified by peer review) is the author/funder, who has granted bioRxiv a license to display the preprint in perpetuity. It is made available under aCC-BY-ND 4.0 International license.

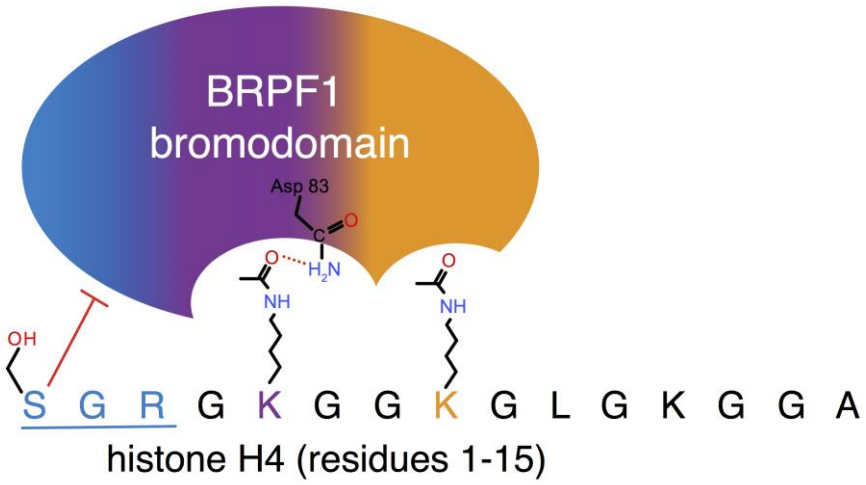

HIGHLIGHTS:

- Histone post-translational modifications recruit bromodomain-containing proteins such as BRPF1 to chromatin, but it is unknown how multiple modifications modulate acetyllysine binding.
- The BRPF1 bromodomain preferentially binds to di-acetyllysine modifications on the histone H4 tail.
- Di-acetyllysine recognition is coordinated by functional monomers of the BRPF1 bromodomain using amino acids near the canonical bromodomain binding pocket.
- Adjacent phosphorylation and methylation modifications on the histone tail inhibit the BRPF1 bromodomain interaction with acetyllysine.
- Cross-talk between multiple modifications on the histone tails is likely an important mechanism for regulating bromodomain interactions with chromatin.

bioRxiv preprint doi: https://doi.org/10.1101/2020.02.13.948091; this version posted February 13, 2020. The copyright holder for this preprint (which was not certified by peer review) is the author/funder, who has granted bioRxiv a license to display the preprint in perpetuity. It is made available under aCC-BY-ND 4.0 International license.

The BRPF1 bromodomain is a molecular reader of di-acetyllysine

Juliet O. Obi[1], Mulu Y. Lubula[1], Gabriel Cornilescu[2], Amy Henrickson[3], Kara McGuire[1], Chiara M. Evans[1], Margaret Phillips[1], Borries Demeler[3], John L. Markley[2] and Karen C. Glass[1*]

[1]Department of Pharmaceutical Sciences, Albany College of Pharmacy and Health Sciences, Colchester, VT 05446, USA

[2]National Magnetic Resonance Facility at Madison and Department of Biochemistry, University of Wisconsin-Madison, Madison, WI 53706, USA

[3]Department of Chemistry and Biochemistry, University of Lethbridge, Lethbridge, Alberta, CA

Keywords: bromodomain, di-acetyllysine, epigenetics, histone, post-translational modification

bioRxiv preprint doi: https://doi.org/10.1101/2020.02.13.948091; this version posted February 13, 2020. The copyright holder for this preprint (which was not certified by peer review) is the author/funder, who has granted bioRxiv a license to display the preprint in perpetuity. It is made available under aCC-BY-ND 4.0 International license.

ABSTRACT

Bromodomain-containing proteins are often part of chromatin-modifying complexes, and their activity can lead to altered expression of genes that drive cancer, inflammation and neurological disorders in humans. Bromodomain-PHD finger protein 1 (BRPF1) is part of the MOZ (monocytic leukemic zinc-finger protein) HAT (histone acetyltransferase) complex, which is associated with chromosomal translocations known to contribute to the development of acute myeloid leukemia (AML). BRPF1 contains a unique combination of chromatin reader domains including two plant homeodomain (PHD) fingers separated by a zinc knuckle (PZP domain), a bromodomain, and a proline-tryptophan-tryptophan-proline (PWWP) domain. BRPF1 is known to recruit the MOZ HAT complex to chromatin by recognizing acetylated lysine residues on the N-terminal histone tail region through its bromodomain. However, histone proteins can contain several acetylation modifications on their N-terminus, and it is unknown how additional marks influence bromodomain recruitment to chromatin. Here, we identify the BRPF1 bromodomain as a selective reader of di-acetyllysine modifications on histone H4. We used ITC assays to characterize di-acetylated histone ligands bound to the BRPF1 bromodomain and found that the domain binds preferentially to histone peptides H4K5acK8ac and H4K5acK12ac. Analytical ultracentrifugation (AUC) experiments revealed that the monomeric state of the BRPF1 bromodomain coordinates di-acetylated histone ligands. NMR chemical shift perturbation studies, along with binding and mutational analysis, revealed non-canonical regions of the bromodomain-binding pocket that are important for histone tail recognition. Together, our findings provide critical information on how the combinatorial action of post-translational modifications can modulate BRPF1 bromodomain binding and specificity.

bioRxiv preprint doi: https://doi.org/10.1101/2020.02.13.948091; this version posted February 13, 2020. The copyright holder for this preprint (which was not certified by peer review) is the author/funder, who has granted bioRxiv a license to display the preprint in perpetuity. It is made available under aCC-BY-ND 4.0 International license.

INTRODUCTION

In the human genome, DNA accessibility and transcriptional activation is often regulated by post-translational modifications (PTMs), among which acetylation of lysine residues on histones plays a major role. Histone acetylation enhances DNA accessibility by loosening the compact conformation of chromatin and by recruiting transcription and chromatin remodeling factors to increase transcriptional activity[1,2]. Bromodomains, which are epigenetic reader domains that specifically recognize ε-N-acetylated lysine residues on histone tails, are known to be important regulators of chromatin remodeling and transcriptional activation[3]. A total of 61 unique bromodomains are known to exist in 46 different bromodomain-containing proteins, and these bromodomains have been grouped into eight major families on the basis of sequence and structural homology[4]. Mutation and aberrant expression of bromodomain-containing proteins has been associated with multiple types of cancer, inflammation, neurological disorders and metabolic diseases. Importantly, bromodomains are often found in chromatin-modifying complexes, whose activity can lead to the altered expression of genes that drive these diseases in humans[5].

Bromodomain-PHD finger protein 1 (BRPF1) is known to play a role in maintaining the expression of genes involved in several developmental processes and hematopoiesis[6-8]. The BPRF1 protein is a unique, multivalent chromatin reader which contains an N-terminal plant homeodomain (PHD)-zinc-knuckle-PHD (PZP) module, a bromodomain for acetyllysine recognition, and a C-terminal proline-tryptophan-tryptophan-proline (PWWP) domain[9]. The N-terminal motif I of BRPF1 interacts with monocytic leukemic zinc finger (MOZ) and MOZ-related factor (MORF), while the downstream motif II interacts with inhibitor of growth 5

bioRxiv preprint doi: https://doi.org/10.1101/2020.02.13.948091; this version posted February 13, 2020. The copyright holder for this preprint (which was not certified by peer review) is the author/funder, who has granted bioRxiv a license to display the preprint in perpetuity. It is made available under aCC-BY-ND 4.0 International license.

(ING5) and the MYST/Esa1-associated factor 6 (MEAF6)[10]. Thus, an important function of BRPF1 is to bridge the association of MOZ and MORF with ING5 and MEAF6, where it is an important regulator of many cellular processes including the self-renewal of leukemic stem cells[8], embryo development and cell proliferation[11], and osteoclast differentiation[12] through its activity with MOZ and MORF[8]. BRPF1 enhances the acetyltransferase activity of the MOZ/MORF HATs via interaction with the histone acetyltransferase domain[10], and also bridges the enzymatic complex to specific post-translational modifications in chromatin[13].

Post-translational modifications (PTMs) on histones are known to be crucial for the regulation of chromatin and DNA accessibility[14]. PTMs modulate signal transduction pathways to recruit effector molecules, such as readers of histone modifications to chromatin[15]. These histone reader domains direct biological outcomes based on the cellular context of the modifications[16]. In humans, proteins are known to undergo a number of PTMs, including but not limited to phosphorylation, methylation, acetylation and ubiquitination, that greatly influence their function in cellular events[17]. Specifically, histone acetylation is an important component of epigenetic signaling, in that it weakens the interactions of histones with DNA by decreasing nucleosome compaction[18], regulates enzymatic activity, and mediates the localization of macromolecular complexes to histones through bromodomain-containing proteins[19]. Therefore, the recognition of acetylated lysine by bromodomains has broad implications for cellular events including chromatin remodeling and transcriptional activation[20].

The postulation that aberrant chromatin acetylation by MOZ may be a contributing factor to the development of cancer and other diseases was first demonstrated by cloning the breakpoint-

bioRxiv preprint doi: https://doi.org/10.1101/2020.02.13.948091; this version posted February 13, 2020. The copyright holder for this preprint (which was not certified by peer review) is the author/funder, who has granted bioRxiv a license to display the preprint in perpetuity. It is made available under aCC-BY-ND 4.0 International license.

associated genes of the recurrent t(8;16)(p11;p13) translocation in patients with a subtype of acute myeloid leukemia (AML)[21]. This translocation results in a novel fusion that combines the PHD finger motifs and MYST acetyltransferase domain of MOZ, with an intact CREB-binding protein (CBP), suggesting that the MOZ-CBP fusion protein gives rise to leukemogenesis through chromatin hyperacetylation[21]. Since BRPF1 plays a crucial role in the MOZ/MORF complex, and their interaction domains remain intact after the translocation, it may also be implicated in the diseases in which MOZ and MORF are known to play a role. The *MOZ* gene has been reported to be mutated in esophageal adenocarcinoma[22], while the *MORF* gene has been reported to be disrupted in leiomyomata[23,24], mutated in familial breast cancer[25], and altered in castration-resistant prostate cancer[26]. Deletion of the mouse *BRPF1* gene showed that BRPF1 is crucial for the growth and proliferation of embryonic fibroblasts and hematopoietic progenitors[11]. Also, multiple mutations in the *BRPF1* gene have been reported to give rise to neurodevelopmental disorders due to a deficiency in histone H3K23 acetylation, supporting evidence that BRPF1 acts through MOZ and MORF to modulate chromatin modification states[7]. The BRPF1 bromodomain belongs to the family IV bromodomains, which also include the BRPF2, BRPF3, BRD7, BRD9, ATAD2 and ATAD2B bromodomains based on their sequence and structural homology[4]. Bromodomains share a conserved globular fold and are composed of a left-handed bundle of four α-helices Z, A, B and C. The helices are linked by loops of variable length (ZA and BC loops), which form the hydrophobic acetyllysine (Kac) binding pocket[4]. The acetyllysine recognition of these bromodomains differ mainly due to the variability within their ZA and BC loops[4].These differences, have also permitted the development of small molecule inhibitors with selectivity for specific bromodomains within the same family[27-30].

bioRxiv preprint doi: https://doi.org/10.1101/2020.02.13.948091; this version posted February 13, 2020. The copyright holder for this preprint (which was not certified by peer review) is the author/funder, who has granted bioRxiv a license to display the preprint in perpetuity. It is made available under aCC-BY-ND 4.0 International license.

An earlier study characterized the interaction of the BRPF1 bromodomain with mono-acetylated ligands on the N-terminal of histone tails, and showed it selects for multiple acetylation modifications including H2AK5ac, H4K12ac and H3K14ac[31]. However, each of the four histone proteins can be post-translationally modified at multiple locations, and with several different chemical marks[32]. Proteomic studies have demonstrated that each histone tail caries a unique set of modifications[33], and that the abundance and availability of specific histone proteoforms is dynamic[34,35]. The BET bromodomains BRD2, BRD4 and BRDT are all able to bind di-acetyllysine modifications including H4K5acK8ac, H4K5acK12ac and H4K12acK16ac[4,36]. Other family IV bromodomains, including the BRD9 and ATAD2 bromodomain, are able to interact with di-acetylated histone ligands such as H4K5acK8ac and H4K5acK12ac, respectively[19,37]. However, it has not been established if the BRPF1 bromodomain can recognize di-acetyllysine modifications, or how multiple histone marks modulate acetyllysine recognition.

Previously published data on the BRPF1 bromodomain revealed that it recognizes several acetylated lysine residues on N-terminal histone tails[31]. Related bromodomain proteins have been observed to cooperatively bind histone peptides with di-acetyllysine marks, through accommodation of the two acetyllysine residues in the same bromodomain binding pocket. For example, the BRDT bromodomain BD1 in the bromodomain and extra-terminal domain (BET) family, recognizes the di-acetylated histone ligand H4K5acK8ac[36]. Other bromodomain proteins in the BET family including BRD2 and BRD4 are also known to recognize di-acetylated histone ligands, mainly through their enlarged binding pockets[4]. Three-dimensional X-ray crystal structures of the BAZ2A and BAZ2B bromodomains in family V have also been solved in complex with H4K16acK20ac and H4K8acK12ac di-acetylated histone ligands[38]. In addition, the

bioRxiv preprint doi: https://doi.org/10.1101/2020.02.13.948091; this version posted February 13, 2020. The copyright holder for this preprint (which was not certified by peer review) is the author/funder, who has granted bioRxiv a license to display the preprint in perpetuity. It is made available under aCC-BY-ND 4.0 International license.

recognition of diacyl-modified histone ligands by the BRD9 bromodomain in family IV has been structurally characterized[19]. However, the binding and recognition of di-acetylated histone ligands by the BRPF1 bromodomain has yet to be fully elucidated.

In this study we characterized the binding affinity of the BRPF1 bromodomain with multiple di-acetylated histone ligands by isothermal titration calorimetry (ITC). We show that the BRPF1 bromodomain binds preferentially to histone peptides H4K5acK8ac and H4K5acK12ac. We utilized nuclear magnetic resonance (NMR) chemical shift perturbation techniques to map the BRPF1 bromodomain binding pocket and identify important residues involved in di-acetyllysine recognition. We performed site-directed mutagenesis experiments, together with ITC and analytical ultracentrifugation (AUC) experiments to evaluate the relative contribution of specific amino acid residues in di-acetyllysine coordination. We also tested how adjacent PTMs impact acetylysine recognition. The results provide new insights on how the BRPF1 bromodomain selects for its di-acetyllysine histone ligands at the molecular level, and how the combinatorial action of post-translational modifications can influence BRPF1 bromodomain binding and specificity. Our study further supports current research efforts geared toward the development of novel therapeutics targeting the BRPF1 bromodomain in acute myeloid leukemia.

RESULTS

The BRPF1 bromodomain recognizes di-acetyllysine histone modifications

We postulated that the BRPF1 bromodomain may be able to recognize di-acetylated histone ligands similarly to the closely related family IV bromodomain BRD9, which has been shown to recognize multiple diacyl modifications on histone H4K5/K8[19]. To investigate our hypothesis,

bioRxiv preprint doi: https://doi.org/10.1101/2020.02.13.948091; this version posted February 13, 2020. The copyright holder for this preprint (which was not certified by peer review) is the author/funder, who has granted bioRxiv a license to display the preprint in perpetuity. It is made available under aCC-BY-ND 4.0 International license.

we sought to further characterize the histone ligands of this bromodomain by performing ITC experiments with mono- and di-acetylated lysine residues on the histone H4 peptide (**Table 1 and Figure 1)**. The mono-acetylated histone H4K5ac peptides (residues 1-10 and 1-15) bound the strongest, out of the mono-acetylated peptides tested, with dissociation constants (K_Ds) of 60.1 ± 6.8 μM and 79.3 ± 4.5 μM. The BRPF1 bromodomain also bound H4K8ac (1-10), H4K12ac (1-15) and H4K16ac (10-20) with K_Ds of 168.4 ± 4.7 μM, 97.3 ± 4.0 μM and 464.3 ± 1.7 μM, respectively. Interestingly, when the ITC experiment was performed with the di-acetylated H4K5acK8ac (1-10) peptide the BRPF1 bromodomain bound with a dissociation constant about two-fold stronger than that of the mono-acetylated H4K5ac peptide (26.7 ± 1.8 μM). Similarly, we found that the combination of H4K5acK12ac marks improved the BRPF1 bromodomain binding affinity six-fold over the recognition for the singly acetylated H4K12ac mark with a K_D of 52.0 ± 2.9 μM, which is also slightly stronger than the single H4K5ac modification. However, other combinations of di-acetylation marks on the histone tail decreased the binding affinity with the BRPF1 bromodomain. The addition of acetylation at lysine 16 in the H4K5acK16ac ligand resulted in a binding affinity of 92.1 ± 7.1 μM, while the H4K8acK16ac bound at 572.8 ± 14.6 μM. The H4K12acK16ac ligand bound with the weakest affinity of 705.6 ± 6.0 μM, while the combination of H4K8acK12ac abrogated the binding interaction.

Interestingly, when compared to our previous results with the BRPF1 bromodomain, inclusion of residues 1-3 on the histone tail also improves the binding interaction with histone H4 peptides that contain the K5 or K8 acetyllysine modification. Thus, the H4K5ac peptides (residues 1-10 or 4-17) bind with K_Ds of 60.1 ± 6.8 μM and 1236 μM, respectively (**Table 1**), while the H4K8ac peptides (residues 1-10 or 4-17) bind with K_Ds of 168.4 ± 4.7 μM and 697 μM,

bioRxiv preprint doi: https://doi.org/10.1101/2020.02.13.948091; this version posted February 13, 2020. The copyright holder for this preprint (which was not certified by peer review) is the author/funder, who has granted bioRxiv a license to display the preprint in perpetuity. It is made available under aCC-BY-ND 4.0 International license.

respectively[31]. However, the peptides with the H4K12ac modification (residues 4-17 or 1-15) had similar binding constants of 86.1 ± 9.1 μM and 97.3 ± 4.0 μM, respectively. This data indicates that residues 1-3 on the N-terminus of histone H4 tail are important for recognition of acetyllysine modifications near the N-terminus of this histone, while recognition of modifications further downstream are not mediated by the N-terminal residues. Furthermore, this is the first direct evidence that the BRPF1 bromodomain can read a span of 8-10 amino acid residues on the histone tail.

Since previous studies have shown that the BRPF1 bromodomain recognizes the H3K14ac histone peptide, we also tested the binding affinity of this bromodomain with mono- and di-acetylated peptides containing the first 24 amino acid residues of human histone H3. Earlier ITC experiments done with the H3K14ac (8-19) and H3K9ac (1-12) peptides had K_Ds of 626 μM, and no binding, respectively [31]. Our current ITC experiments on the H3K14ac (1-24) and H3K9ac (1-24) peptides revealed that these ligands have dissociation constants of 182.7 μM and 751.1 μM, respectively. A dissociation constant of 233.8 μM was obtained for the H3K9acK14ac (1-24) di-acetylated histone peptide, which indicates that the acetylation mark at K9 impairs the ability of the BRPF1 bromodomain to bind H3K14ac (**Table 1, Figure 1).** Taken together, our results in **Table 1** show that the BRPF1 bromodomain is able to recognize di-acetyllysine modifications over a span of 8-10 amino acids on the histone tail, which suggests it may be important for the effector-mediated recognition of histone proteins bearing multiple modifications.

bioRxiv preprint doi: https://doi.org/10.1101/2020.02.13.948091; this version posted February 13, 2020. The copyright holder for this preprint (which was not certified by peer review) is the author/funder, who has granted bioRxiv a license to display the preprint in perpetuity. It is made available under aCC-BY-ND 4.0 International license.

Thermodynamics of di-acetylated histone ligand binding to the BRPF1 bromodomain

To further understand the binding mechanism driving recognition of mono- and di-acetylated histone ligands by the BRPF1 bromodomain, we investigated the thermodynamic parameters obtained from our ITC data. The ΔH and ΔS values calculated for the BRPF1 bromodomain interaction with various mono- and di-acetylated histone ligands are shown in **Table 1**, and reflect how the enthalpic and the entropic terms contribute to the binding affinity (K_D). Larger, negative changes in enthalpy (ΔH) were observed upon binding of the di-acetylated histone ligands to the BRPF1 bromodomain as compared to the mono-acetylated histone ligands. Amongst the di-acetylated histone ligands, H4K5acK8ac (1-10) and H4K5acK12ac (1-15) showed not only the most negative ΔH values, but also the highest binding affinities K_D = 26.7 ± 1.8 μM and 52.0 ± 2.9 μM, respectively, indicating that more energetically favorable electrostatic and van der Waals interactions form with these ligands. The change in entropy (ΔS) to more negative values observed upon BRPF1 bromodomain binding to the di-acetylated histone ligands is also suggestive of favorable conformational changes that occur during the complex formation. In contrast, the mono-acetylated histone ligands showed more positive ΔH values and ΔS values, supporting a less favorable interaction of these peptides with the BRPF1 bromodomain.

Crosstalk between PTMs modulate acetyllysine recognition by the BRPF1 bromodomain

To determine how the combinatorial action of PTMs on the histone tail modulates acetyllysine recognition, we performed ITC experiments to observe how the *in vitro* binding affinity of the BRPF1 bromodomain for acetylated histone peptides would change if other modifications are located adjacent to the acetyllysine (Kac) recognition site (**Table 1 and Figure 1**). The BRPF1

bioRxiv preprint doi: https://doi.org/10.1101/2020.02.13.948091; this version posted February 13, 2020. The copyright holder for this preprint (which was not certified by peer review) is the author/funder, who has granted bioRxiv a license to display the preprint in perpetuity. It is made available under aCC-BY-ND 4.0 International license.

bromodomain recognized the H4K5ac (1-15) mono-acetylated histone peptide with a binding affinity of 79.3 μM, but binding decreased by approximately three-fold (K_D = 228.5 μM) when serine 1 of histone H4 was phosphorylated. The BRPF1 bromodomain also recognizes the H4K12ac (1-15) peptide with a binding affinity of 97.3 μM, and the affinity is decreased by ~1.5-fold (169.6 μM) when lysine 5 was tri-methylated. Interestingly, tri-methylation of lysine 12 in combination with acetylation of lysine 5 did not significantly alter the affinity of the BRPF1 bromodomain for the H4K5ac (1-15) histone ligand, indicating that the H4K12me3 mark is permissive for H4K5ac recognition. Together, our results show that crosstalk between adjacent PTMs on the histone tail modulate how acetyllysine is recognized by the BRPF1 bromodomain.

The BRPF1 bromodomain recognizes di-acetylated histone ligands as a monomer

As shown in **Table 1**, the N value observed in all of our ITC data indicates that the BRPF1 bromodomain interacts with modified histone H3 and H4 tails as a monomer. To confirm this, we also performed analytical ultracentrifugation sedimentation velocity experiments to determine the molecular mass of this bromodomain in complex with mono- and di-acetylated histone ligands. The molecular weight of the apo BRPF1 bromodomain is 13,703 Da, while the molecular weights of the histone ligands tested range from 958-1371 Da. Strikingly, the signal peaks of the BRPF1 bromodomain alone, or in complex with its mono- and di-acetylated histone ligands, overlap at approximately 14-15 kDa (**Figure 2**). These results support our ITC data showing that the BRPF1 bromodomain recognizes both mono- and di-acetylated histone ligands as a monomer in solution.

bioRxiv preprint doi: https://doi.org/10.1101/2020.02.13.948091; this version posted February 13, 2020. The copyright holder for this preprint (which was not certified by peer review) is the author/funder, who has granted bioRxiv a license to display the preprint in perpetuity. It is made available under aCC-BY-ND 4.0 International license.

Characterization of the BRPF1 bromodomain binding pocket by NMR

To outline specific amino acid interactions in the BRPF1 bromodomain binding pocket with the mono- and di-acetylated histone peptides, two-dimensional, ^{1}H-^{15}N heteronuclear single quantum coherence (HSQC) NMR experiments were performed. We previously reported the backbone assignments for the BRPF1 bromodomain accomplished by means of multidimensional NMR spectroscopy[31]. Here, the amide-NH chemical shift perturbations induced in the residues of the BRPF1 bromodomain sample were monitored upon the addition of acetylated histone peptides H4K5ac (1-10), H4K8ac (1-10), H4K12ac (4-17), H4K5ac (1-15) as well as the di-acetylated histone ligands H4K5acK8ac (1-10) and H4K5acK12ac (1-15) at increasing concentrations until the saturation point was observed. The bar graphs in **Figures 3A-F** show the normalized chemical shift changes of individual residues in the BRPF1 bromodomain upon addition of the respective mono- and di-acetylated histone peptides, in a 1:5 molar ratio. To rule out non-specific interactions we determined the most significant chemical shift perturbations by calculating the standard deviation (σ) of the Euclidean chemical shift change for all ligands. Residues with chemical shift changes > 2σ are highlighted in red, while residues with chemical shift changes > 1σ and > 0.5σ are indicated in orange and yellow. The affected amino acids were then mapped onto the surface of the apo BRPF1 bromodomain crystal structure (PDB ID: 2D9E) and it was observed that the majority of the altered resonances with large chemical shifts come from residues clustered around the acetyllysine binding pocket (**Figure 3A-F**). Residues I27, L34, E36, V37, N83 and I88 consistently showed the largest chemical shift perturbations upon addition of mono- and/or di-acetylated peptides. A few of chemical shift perterbations also come from residues found more peripherally to the binding pocket. Amino acids including L9, I10, L11, Q55 and N56, which are located distal to the

bioRxiv preprint doi: https://doi.org/10.1101/2020.02.13.948091; this version posted February 13, 2020. The copyright holder for this preprint (which was not certified by peer review) is the author/funder, who has granted bioRxiv a license to display the preprint in perpetuity. It is made available under aCC-BY-ND 4.0 International license.

acetyllysine binding pocket, demonstrated chemical shift perturbations due to conformational changes within the bromodomain that occur in response to ligand binding. Minimal chemical shift perturbations were seen with the H4K8ac (1-10) histone ligand with only G36 and N83 showing significant perturbations, thus indicating weak binding of the histone H4K8ac ligand to the BRPF1 bromodomain. This is also supported by our ITC experiment (**Table 1, Figure 1**) in which a lower binding affinity (K_D = 168.4 ± 4.7 μM), and a higher unfavorable entropy change, was observed for binding of the histone H4K8ac peptide.

Mutational analysis identifies residues that may coordinate the second acetyllysine moiety

To obtain more information about coordination of di-acetyllysine by the BRPF1 bromodomain we used site-directed mutagenesis coupled to ITC binding assays (**Table 2 and supplemental Fig S1**). To investigate whether both acetyllysine groups in the di-acetylated histone ligands are accommodated in the canonical BRPF1 bromodomain binding pocket, or if secondary binding contacts exist on the BRPF1 bromodomain, we carefully chose six amino acid residues (T24, N26, E30, E36, K81, R91) to mutate to alanine. Amino acid residues T24 and R91 were mutated to test the possibility of an additional binding surface that was shown to coordinate H3K14ac between the αZ and αC helices as observed for the ATAD2 bromodomain[39]. N26 was mutated to probe the differences in its chemical shift perturbation pattern in the presence of the mono-acetylated H4K5ac (1-15) ligand versus the di-acetylated H4K5acK12ac (1-15) ligand in our NMR chemical shift data (**Figure 3E-F**). E30 was chosen based on its proximity to the N-1,3-dimethyl-2-oxo-6-(piperidin-1- yl)-2,3-dihydro-1H-1,3-benzodiazol-5-yl-2-methoxybenzamide small molecule inhibitor seen in the acetyllysine binding site of the BRPF1 bromodomain crystal structure 4UYE[40]. E36 was predicted to make side chain interactions with lysine 8 on histone H4

bioRxiv preprint doi: https://doi.org/10.1101/2020.02.13.948091; this version posted February 13, 2020. The copyright holder for this preprint (which was not certified by peer review) is the author/funder, who has granted bioRxiv a license to display the preprint in perpetuity. It is made available under aCC-BY-ND 4.0 International license.

during a molecular dynamic simulation of the ATAD2 bromodomain in complex with the H4K5acK12ac ligand[41]. Lastly, the K81 residue was mutated because of its proximity to lysine 8 in our published structure of the BRPF1 bromodomain in complex with its H4K12ac ligand (PDBID: 4QYD)[42]. We performed circular dichroism (CD) experiments on the mutant BRPF1 bromodomain proteins (**Table 3 and Figure 4**) to ensure they were properly folded, and we ran ITC binding experiments to test the binding affinities of the BRPF1 bromodomain mutants in combination with H4K5ac (1-10), H4K12ac (1-15), H4K5acK8ac (1-10) and H4K5acK12ac (1-15) histone ligands. These experiments were designed to test our hypothesis that if the second acetyllysine group is coordinated via specific side-chain interactions on the BRPF1 bromodomain, then mutating it should decrease the binding affinity to what is seen for the singly acetylated histone ligands. The binding affinities with observed stoichiometries of the mutant BRPF1 bromodomains for the histone ligands tested are shown in **Table 2**. The ITC traces of the mutant BRPF1 bromodomains with their histone ligands are located in **Supplemental Figure S1**. Interestingly, all of the alanine mutations to the BRPF1 bromodomain caused an increase in binding affinity for the H4K5acK12ac ligand, while most of these mutations caused at least a slight decreased in binding affinity for H4K5acK8ac. Our mutational study did not cause the binding affinity of di-acetylated ligands to revert to singly acetylated ligand values, but the T24A, E36A and K81A mutations did show a weakened binding interaction between the BRPF1 bromodomain and the H4K5acK8ac ligand. The N26A mutation decreased the affinity for the H4K12ac (1-15) ligand. and increased the binding affinity for the H4K5acK12ac (1-15) and H4K5ac (1-10) ligands, but it did not have a large effect on binding of the H4K5acK8ac (1-10) ligand. The remaining mutations either caused no significant difference in the binding interaction, or resulted in increased binding affinities with the BRPF1 bromodomain. The

bioRxiv preprint doi: https://doi.org/10.1101/2020.02.13.948091; this version posted February 13, 2020. The copyright holder for this preprint (which was not certified by peer review) is the author/funder, who has granted bioRxiv a license to display the preprint in perpetuity. It is made available under aCC-BY-ND 4.0 International license.

inconsistent binding affinity of BRPF1 mutants suggests that multiple residues are involved in coordinating the second acetyllysine group.

The role of ordered water in bromodomain structure and histone ligand coordination

We made a conservative change to Y40 by mutating the residue to a phenylalanine in order to investigate how loss of water coordination would impact acetyllysine recognition. The BRPF1 Y40F bromodomain variant was unable to bind mono- or di-acetylated histone ligands (**Table 2 and Figure 5)**, and surprisingly loss of the ordered water molecule also resulted in significant changes in the bromodomain secondary structure. As seen in **Table 3**, the alpha helical content of the BRPF1 Y40F bromodomain mutant was reduced from 94% to 43%, while the beta strand content increased from almost zero to 18%. Thus, it appears that ordered water in the bromodomain binding pocket is not only important for the recognition of acetylated histone ligands, but it also plays a key role in maintaining the 3D fold of the bromodomain module.

DISCUSSION

Previous studies on the BRPF1 bromodomain revealed that it recognizes several acetylated lysine residues on the N-terminus of histone tails[31]. The BRPF1 bromodomain preferentially selects for acetylation modifications on the histone H4 tail, including histone H4 acetylated at lysine 5 (H4K5ac), and lysine 8 and lysine 12 (H4K8ac and H4K12ac). However, BRPF1 is also able to recognize the histone H3 and H2A ligands H3K14ac and H2AK5ac[31]. More recently it has been discovered that bromodomain-containing proteins such as BRD2, BRD3 and BRD4 can bind to histone ligands with di-acetyllysine marks[43]. Another example of this is the first bromodomain (BD1) in the bromodomain testis specific protein (BRDT), which is a member of

bioRxiv preprint doi: https://doi.org/10.1101/2020.02.13.948091; this version posted February 13, 2020. The copyright holder for this preprint (which was not certified by peer review) is the author/funder, who has granted bioRxiv a license to display the preprint in perpetuity. It is made available under aCC-BY-ND 4.0 International license.

the bromodomain and extra-terminal domain (BET) subfamily. BRDT BD1 failed to recognize mono-acetylated histone H4 tails, but was able to bind multiple di-acetylated histone H4 peptides as well as tetra-acetylated histone H3 peptides[36]. BRDT BRD1 recognizes the di-acetylated histone ligand H4K5acK8ac with a low micromolar affinity, and the crystal structure of the BRDT BD1 in complex with this ligand demonstrated the 'wide pocket' of the BRDT BD1 bromodomain is able to accommodate both acetylated lysine residues within the canonical bromodomain binding pocket[36]. This is opposed to the 'keyhole pocket' of the yeast GCN5 bromodomain, which is only able to fit one acetyllysine group inside the binding pocket at a time. Coordination of di-acetyllysine by the first bromodomain in the BET subfamily appears to be conserved as demonstrated by ligand binding assays with BRD1 and BRD2[44,45], as well as structures of BRD4 BD1 with H4K5acK8ac and H4K12acK16ac (PDBIDs 3UVW and 3UVX, respectively)[4]. It has been suggested that other bromodomain protein families can recognize di-acetylated histone ligands as well, possibly through alternative binding modes. The structures of the BAZ2A and BAZ2B bromodomains have been solved with the di-acetylated histone H4 ligands H4K16acK20ac and H4K8acK12ac, respectively (PDBIDs 4QBM and 4QC3)[38]. In these structures, BAZ2A is able to coordinate the di-acetylated ligand as a monomer, much like the BET family bromodomains, while the BAZ2B bromodomain forms a dimeric complex to coordinate the H4K8acK12ac histone ligand.

In this study, we show the BRPF1 bromodomain is able to selectively recognizes multiple histone mark combinations and binds preferentially binds to di-acetylated ligands on the N-terminus of histone H4. The results from our ITC binding assays demonstrate that this bromodomain is capable of recognizing several di-acetylated histone ligands and has the highest

bioRxiv preprint doi: https://doi.org/10.1101/2020.02.13.948091; this version posted February 13, 2020. The copyright holder for this preprint (which was not certified by peer review) is the author/funder, who has granted bioRxiv a license to display the preprint in perpetuity. It is made available under aCC-BY-ND 4.0 International license.

affinity for the histone H4K5acK8ac ligand, followed by the H4K5acK12ac ligand. Our results also show that the interaction of the BRPF1 bromodomain interaction with histone ligands is enthalpy-driven. A similar result was also observed for the BRPF1 bromodomain with small-molecule ligands, and with the ATAD2 bromodomain-ligand complexes[46,47]. The enthalpy (ΔH) and entropy (ΔS) changes obtained from fitting the binding isotherm illustrate the mechanism driving the protein–ligand interaction[48]. A tight binding interaction typically arises from several favorable associations (mostly noncovalent) between the protein and the ligand, thus resulting in a large negative change in enthalpy while also accompanied by a negative entropy change due to restricted mobility of the interacting partners[48,49]. Thus, the larger, more negative enthalpy and entrophy changes induced upon binding to the H4K5acK8ac and H4K5acK12ac ligands, as compared with the mono-acetylated ligands, supports the formation of a stronger, more stable complex with these ligands.

We also tested the histone H4K5acK16ac and H4K8acK16ac ligands and found that these di-acetyllysine combinations weakened the BRPF1 bromodomain interaction with the histone tail. Examination of the histone H3/H4 proteoforms found in human cancer cell lines revealed that in promyelocytic leukemia cells (HL60) the H4K5acK16ac mark is down-regulated, while it is up-regulated in acute promyelocytic (NB4) cells[50]. Additionally, the H4K8acK16ac mark was down-regulated in all leukemia cell lines tested. Thus, as histone PTMs are altered in disease states, the availability of particular acetyllysine combinations will enhance or inhibit the interaction of BRPF1 with chromatin and influence recruitment of the MOZ/MORF HAT complex.

bioRxiv preprint doi: https://doi.org/10.1101/2020.02.13.948091; this version posted February 13, 2020. The copyright holder for this preprint (which was not certified by peer review) is the author/funder, who has granted bioRxiv a license to display the preprint in perpetuity. It is made available under aCC-BY-ND 4.0 International license.

Results from our previous study demonstrated that the BRPF1 bromodomain recognizes the singly-acetylated histone ligands H2AK5ac, H4K12ac, H4K8ac, H4K5ac and H3K14ac respectively[31]. Our current results demonstrate the BRPF1 bromodomain preferentially binds to the H4K5ac modification on singly acetylated histones, which is likely the predominant interaction driving recognition of di-acetylated ligands. Interestingly, the ITC binding data show that the BRPF1 bromodomain functions as a di-acetyllysine reader, with a binding pocket able to recognize PTMs over span of 8-10 residues on each histone tail. Additionally, the BRPF1 bromodomain interacts with mono- and di-acetylated histone ligands as a monomer in solution based on the binding stoichiometry (N: peptide-to-bromodomain ratio) observed in the ITC binding assays and confirmed in AUC experiments. A study on the family IV BRD9 bromodomain indicated that it binds to the histone H4K5acK8ac ligand with an ITC N-value of 0.44, suggesting a dimeric interaction with two bromodomains bound to one histone peptide[19]. The family IV bromodomains possess a "keyhole style" pocket due to a larger aromatic gatekeeper residue that can only accommodate one acetyllysine group in the canonical binding site[19,36]. Thus, in ITC binding assays and crystallization studies the BRD9 bromodomain interacts with the di-acetylated histone ligand by coordinating the H4K5ac group in one bromodomain with the H4K8ac site bound to a second bromodomain module (PDBID: 4YYI)[19]. A related structure shows that the BRPF1 bromodomain binds to the histone H4K5acK8ac in an identical manner as an apparent dimer (PDBID: 5FFW)[12]. However, this is likely due to crystal packing effects caused by the crystallization conditions used for solving the crystal structure, since our ITC binding data and analytical ultracentrifugation analysis of the BRPF1 bromodomain support monomeric coordination of both mono- and di-acetylated histone ligands in solution. Also, unlike the BET proteins, which contain two adjacent bromodomain modules[51],

bioRxiv preprint doi: https://doi.org/10.1101/2020.02.13.948091; this version posted February 13, 2020. The copyright holder for this preprint (which was not certified by peer review) is the author/funder, who has granted bioRxiv a license to display the preprint in perpetuity. It is made available under aCC-BY-ND 4.0 International license.

the BRPF1 protein has only one bromodomain, and this protein functions as a single subunit within the MOZ/MORF HAT complexes[4,10]. Thus, the BRPF1 bromodomain is likely to be monomeric in its biologically active form.

Histone H4 can be post-translationally modified at multiple positions and is frequently acetylated at lysine 5, 8, 12 and 16. It also often carries a phosphorylation mark on serine 1, as well as methyl groups on arginine 3 and lysine 20[52]. The SET-domain methyltransferases performs methylation of lysine on the histone tails[53], which can be mono-, di- or tri-methylated. Lysine at position 5 and 12 of histone H4 can also be methylated[32,54]. Since acetylation at lysine 5 and 12 on histone H4 are the positions the BRPF1 bromodomain binds with highest affinity, we tested the effect tri-methylation at these sites would have on bromodomain binding. Our results demonstrated that tri-methylation of H4K5 reduced the binding affinity of the BRPF1 bromodomain for the H4K12ac ligand, while tri-methylation of H4K12 did not have a significant impact on the recognition of H4K5ac. We also characterized how phosphorylation of serine 1 modulates the acetyllysine binding activity of the BRPF1 bromodomain and showed that this mark has an inhibitory effect on recognition of H4K5ac. Histone phosphorylation has previously been linked to DNA damage repair mechanisms[55], and H4S1phos is known to be enriched 20- to 25-fold in nucleosomes that are located adjacent to double strand breaks[56]. The impact of modifications adjacent to acetyllysine recognition sites may be biologically relevant to BRPF1's function in recruiting the MOZ HAT tetrameric complex to distinct sites on chromatin depending on the epigenetic landscape. For example, phosphorylation of histone H4S1 at sites of DNA damage could function to prevent or delay the transcriptional activation signaling by acetylation modifications until the genetic information can be repaired. Therefore, our study represents an

bioRxiv preprint doi: https://doi.org/10.1101/2020.02.13.948091; this version posted February 13, 2020. The copyright holder for this preprint (which was not certified by peer review) is the author/funder, who has granted bioRxiv a license to display the preprint in perpetuity. It is made available under aCC-BY-ND 4.0 International license.

important first step in understanding how the BRPF1 bromodomain is able to recognize and bind di-acetyllysine on the histone tail, and how cross-talk among adjacent marks influences its activity.

To delineate the acetyllysine binding site on BRPF1 bromodomain we used NMR chemical shift perturbation data to identify the residues involved in di-acetyllysine recognition, and to observe whether residues outside the canonical acetyllysine binding pocket are important for coordinating the second acetyllysine modification. Interestingly, our NMR titration analysis displayed a similar trend in the chemical shift perturbations observed for the mono- versus the di-acetylated histone ligands. The reason for this could be two-fold: Firstly, in the present *in-vitro* condition, the BRPF1 bromodomain shows a similar binding pocket for the mono- versus the di-acetylated H4 histone ligands, thus indicating that there may be other mechanisms involved in more specific interactions of the BRPF1 bromodomain with the di-acetylated H4 histone tail *in-vivo*. BRD7, which shows high structural similarity to BRPF1, has also been reported to lack specificity towards histone ligands in *in-vitro* conditions[57]. Secondly, the second acetyllysine is likely making transient side chain interactions with certain residues surrounding the canonical BRPF1 bromodomain binding pocket not readily detected by our backbone amide NMR titrations. A similar observation was made for the BRDT BD1 bromodomain, which interacts with the di-acetylated H4K5acK8ac histone ligand via the methyl groups of the hydrophobic residues lining the bromodomain pocket[36].

Large chemical shift perturbations for the N83 residue of BRPF1 bromodomain were consistently observed in our NMR titration analysis confirming the importance of this residue in

bioRxiv preprint doi: https://doi.org/10.1101/2020.02.13.948091; this version posted February 13, 2020. The copyright holder for this preprint (which was not certified by peer review) is the author/funder, who has granted bioRxiv a license to display the preprint in perpetuity. It is made available under aCC-BY-ND 4.0 International license.

the coordination of acetylated H4 histone peptides. When compared to the crystal structure of the BRDT BD1 in complex with H4K5acK8ac (1-20) (PDBID:2WP2), the BRPF1 bromodomain (PDBID:2D9E) seems to adapt a similar binding environment for the H4K5ac moiety as the BD1 bromodomain (**Supplementary Figure S2**). Mainly, in the BRDT BD1, residues V55, L62 and C104 are known to be involved in hydrophobic interactions with the H4K5ac moiety in addition to the hydrogen bond with N108[36]. In BRPF1, these correspond to residues V32, V37 and C79 as well as to the conserved N83 residue, based on their structural alignment (RMSD = 1.755) determined using the protein structure comparison service PDBeFold at the European Bioinformatics Institute (http://www.ebi.ac.uk/msd-srv/ssm)[58]. The same residues also showed chemical shift perturbations for di-acetylated histone H4 ligands (H4K5acK8ac and H4K5acK12ac) indicating that the K5ac group interacts with the BRPF1 bromodomain in the same position regardless of the second acetyllysine site on the histone.

We introduced additional mutations into the BRPF1 bromodomain binding pocket to test hypotheses based on previous studies of acetyllysine coordination by other related bromodomains[39-42]. I27 is found in the BRPF1 "NIF Shelf", which is important for ligand selectivity[59]. L34, E36 and V37 are all located in the flexible ZA loop adjacent to the acetyllysine binding site, which is predicted to be important for increasing the on-rate of histone tail binding[41]. N83 is the universally conserved asparagine residue involved in coordination of the acetyllysine modification on histones[59]. I88 is adjacent to the 'gatekeeper' residue F89 (unassigned) that lines the acetyllysine binding pocket. We used ITC experiments with a subset of the histone H4 peptides to compare the binding activity of the mutant BRPF1 bromodomain proteins with the affinities measured for the WT BRPF1 bromodomain (**Table 2**). Circular

bioRxiv preprint doi: https://doi.org/10.1101/2020.02.13.948091; this version posted February 13, 2020. The copyright holder for this preprint (which was not certified by peer review) is the author/funder, who has granted bioRxiv a license to display the preprint in perpetuity. It is made available under aCC-BY-ND 4.0 International license.

dichroism spectroscopy studies were also carried out to ensure that the mutations had no significant effect on the overall structure of the BRPF1 bromodomain. Residue E36 in the BRPF1 bromodomain showed the largest chemical shift perturbation upon addition of either mono- or di-acetylated histones. Alignment of the apo crystal structure of the BRPF1 bromodomain (PDBID: 2D9E) with BRPF1 bromodomain structures in combination with the H2AK5ac and H4K12ac ligands (PDBIDs: 4QYL and 4QYD)[42], demonstrate that the E36 residue does not contact the histone ligands directly, but undergoes a large conformational change as part of the ZA loop to accommodate peptide binding. Mutation of E36 to alanine does not significantly alter the binding affinity of the BRPF1 bromodomain with the H4K5ac (1-10) ligand, but it does decrease the interaction of BRPF1 with the di-acetylated histone H4K5acK8ac (1-10) ligand (**Table 2**), suggesting it may be an important contact for the K8ac moiety. A recent study investigating the intermolecular contacts between the related ATAD2 family IV bromodomain and the H4K5acK12ac ligand found that residue E1017, which is equivalent to E36 in the BRPF1 bromodomain, comes within 5Å of H4K8 in molecular dynamic simulations of the holo complex[41].

A prior study on the ATAD2 bromodomain found the H3K14ac ligand bound to a secondary site distal from the canonical bromodomain binding site[39]. In this ATAD2 structure (PDBID: 4TT4), two residues were involved in coordination of the acetyllysine moiety, R1005 and H1076. H1076 is equivalent to T24 in the BRPF1 bromodomain. The T24A mutant showed a two-fold stronger binding affinity for the H4K5ac (1-10) ligand than the wild-type BRPF1 bromodomain, while also having a weaker interaction with the H4K5acK8ac (1-10) ligand. This suggests that residue T24 plays some role in coordinating either the K5ac or the K8ac in the di-acetylated

bioRxiv preprint doi: https://doi.org/10.1101/2020.02.13.948091; this version posted February 13, 2020. The copyright holder for this preprint (which was not certified by peer review) is the author/funder, who has granted bioRxiv a license to display the preprint in perpetuity. It is made available under aCC-BY-ND 4.0 International license.

histone ligand. Notably, mutation of either K81 to alanine significantly weakened the interaction of the BRPF1 bromodomain for the H4K5acK8ac ligand, also indicating a role for this residue in coordination of this di-acetylated histone ligand. However, the N26A and E30A mutations resulted in modest changes in the binding affinity of the BRPF1 bromodomain for the histone ligands, suggestive of the neutral role of these residues in acetyllysine binding. Similarly, the R91A mutation resulted in slightly stronger binding interactions of the BRPF1 bromodomain with both the mono- and di-acetyllysine ligands. When the histone peptides contain two acetyllysine groups it is possible for either group to be inserted into the canonical bromodomain binding pocket. One possible reason we observed an increase in binding affinity of the mutant BRPF1 bromodomain proteins with the di-acetyllysine ligands could be because their binding is now stabilized in one orientation over the other. In a di-acetylated ligand, not only is each acetyllysine group able to insert into the canonical binding pocket, but the peptide can bind in different orientations (e.g. from N- to C-terminal or vice versa) across the surface of the bromodomain binding pocket. Thus, by altering the BRPF1 bromodomain surface contacts with histone residues surrounding the primary acetyllysine inserted into the canonical binding pocket, some of our mutations may be preferentially selecting for one orientation over another, thereby stabilizing the ligand binding interaction with both mono- and di-acetylated histone peptides. Overall, our NMR titration and mutagenesis data demonstrate that the acetyllysine binding pocket in BRPF1 bromodomain binds a variety of acetylated histone ligands with a conserved binding mechanism, and that increased sidechain and/or hydrophobic interactions are involved in the coordination of the second acetyllysine group, thus resulting in stronger binding affinities for the di-acetylated histone ligands.

bioRxiv preprint doi: https://doi.org/10.1101/2020.02.13.948091; this version posted February 13, 2020. The copyright holder for this preprint (which was not certified by peer review) is the author/funder, who has granted bioRxiv a license to display the preprint in perpetuity. It is made available under aCC-BY-ND 4.0 International license.

Previous studies have identified ordered waters in the bromodomain binding pocket that coordinate the acetyllysine modification[42,60]. One of these waters (w1) connects the carbonyl oxygen of the acetyllysine moiety to the hydroxyl group of Y40. Y40 is located in the αAZ loop of the bromodomain module and sequence alignment reveals that this tyrosine is conserved in all but two of the human bromodomain proteins[4], thus this residue is even more highly conserved than the binding site asparagine residue that contacts the acetyllysine group directly. Our conservative mutation of this residue to phenylalanine demonstrated that not only is Y40 essential for water coordination, but it also plays an important structural role supporting the three-dimensional fold of the bromodomain module. Our results shed light on why Y40 is the most highly conserved amino acid residue found in human bromodomains.

In summary, we characterized the di-acetylated histone ligands of the BRPF1 bromodomain, and our results demonstrate that the BRPF1 bromodomain is able to recognize multiple acetyllysine combinations on the histone tail. Our results also confirm that cross-talk between PTMs on histone tail peptides can modulate acetyllysine recognition by the BRPF1 bromodomain. This research provides further insights into how the BRPF1 bromodomain recruits its partners in the MOZ/MORF HAT complexes to chromatin, with different combinations of PTMs either promoting or inhibiting the binding interaction. Chromosomal translocations of the MOZ HAT are associated with acute myeloid leukemia, and fusion of MOZ with TIF2, CBP and p300 are thought to drive leukemogenesis through aberrant acetylation[61-63]. Understanding how cross-talk influences bromodomain binding specificity and affinity is an important first step to connect how epigenetic changes contribute to the etiology of disease, and may provide new mechanisms for therapeutic intervention in the treatment of AML and other diseases.

bioRxiv preprint doi: https://doi.org/10.1101/2020.02.13.948091; this version posted February 13, 2020. The copyright holder for this preprint (which was not certified by peer review) is the author/funder, who has granted bioRxiv a license to display the preprint in perpetuity. It is made available under aCC-BY-ND 4.0 International license.

MATERIALS AND METHODS

Plasmid construction

The cDNA coding for human BRPF1 was kindly provided to us by Dr. Xiang-Jiao Yang at McGill University. Residues 629-742 encoding the BRPF1 bromodomain region were amplified using PCR and subsequently cloned into the pDEST15 vector encoding an N-terminal glutathione S-transferase (GST) tag. The Gateway cloning technology (Invitrogen) was used for cloning the BRPF1 bromodomain as described previously [31]. BRPF1 bromodomain mutants T24A, N26A, E30A, E36A, Y40F, K81A and R91A were generated using the QuikChange® mutagenesis procedure (Stratagene) as described previously [64]. All of the mutants were also cloned into the pDEST15 vector and the DNA sequences of the wild-type (WT) and mutant proteins were verified by Eurofins Genomics. The WT and mutant plasmids were then transformed into *Escherichia coli* Rosetta™ 2(DE3)pLysS competent cells (Novagen) for protein expression.

BRPF1 bromodomain expression and purification

E. coli Rosetta™ 2(DE3)pLysS cells expressing the WT and mutant GST-tagged BRPF1 bromodomain were grown in terrific broth (TB) at 37°C until an OD_{600} of 1.0 was reached. The temperature was reduced to 16°C for 1 h, and the cultures were induced by 0.25 mM isopropyl β-D-1-thiogalactopyranoside (IPTG) and incubated overnight for over 16 h at 16°C. The cells were harvested by centrifugation and sonicated after resuspension in lysis buffer (50 mM Tris pH 7.5, 150 mM NaCl, 0.05% Nonidet P-40 and 1mM DTT) containing 0.1 mg/mL lysozyme (Thermo Scientific). After centrifugation at 10,000 RPM, the cell supernatant was mixed with glutathione agarose resin (Thermo Scientific) and incubated on ice (4°C) for 2 h while agitating. The BRPF1 bromodomain protein was purified on glutathione agarose resin in a 25 mL Econo-Column®

bioRxiv preprint doi: https://doi.org/10.1101/2020.02.13.948091; this version posted February 13, 2020. The copyright holder for this preprint (which was not certified by peer review) is the author/funder, who has granted bioRxiv a license to display the preprint in perpetuity. It is made available under aCC-BY-ND 4.0 International license.

(Bio-Rad) by first washing the beads extensively with wash buffer containing 20 mM Tris pH 8.0, 150 mM NaCl and 1 mM DTT. The GST tag was cleaved overnight at 4°C by addition of PreScission Protease (GE Healthcare), and the BRPF1 bromodomain was eluted with wash buffer. The eluted fractions were pooled, concentrated to approximately 3 mL, and dialyzed into appropriate buffers. For NMR experiments the ^{15}N-labeled BRPF1 bromodomain was expressed and purified as previously described [31]. The uniformly ^{15}N-labeled BRPF1 bromodomain was prepared at a concentration of 0.4 mM in 20 mM Tris-HCl pH 6.8, 150 mM NaCl and 10 mM DTT with 10% D_2O added to the sample. For ITC and circular dichroism (CD) experiments, the purified BRPF1 bromodomain was dialyzed, respectively, into ITC buffer (20 mM NaH_2PO_4 pH 7.0, 150 mM NaCl and 1 mM TCEP), or CD buffer (50 mM NaH_2PO_4 pH 7.0, 50 mM NaCl). For analytical ultracentrifugation (AUC) experiments, the protein was further purified over a gel filtration column (HiPrep 16/60 Sephacryl S-100 High Resolution, GE Healthcare) equilibrated with AUC buffer (50 mM NaH_2PO_4 pH 7.0, 50 mM NaCl and 1 mM TCEP) via fast-protein liquid chromatography. The concentration of the BRPF1 bromodomain was calculated from optical absorbance measurements with the A_{280} = 7450 M^{-1} cm^{-1}. The purity of the BRPF1 bromodomain was verified by SDS-polyacrylamide gel electrophoresis stained with GelCode Blue Safe protein stain (Thermo Scientific).

Histone peptide synthesis

Histone peptides containing unique acetylated and/or methylated lysine, as well as phosphorylated serine modifications were synthesized by GenScript and purified by HPLC to 98% purity. The correct composition of each peptide was confirmed by mass spectrometry.

bioRxiv preprint doi: https://doi.org/10.1101/2020.02.13.948091; this version posted February 13, 2020. The copyright holder for this preprint (which was not certified by peer review) is the author/funder, who has granted bioRxiv a license to display the preprint in perpetuity. It is made available under aCC-BY-ND 4.0 International license.

Isothermal titration calorimetry

ITC measurements were conducted using a MicroCal iTC200 instrument (Malvern Panalytical). All experiments were performed at 5°C. The BRPF1 WT and mutant bromodomain proteins were dialyzed into ITC buffer containing 20 mM NaH_2PO_4 pH 7.0, 150 mM NaCl and 1 mM TCEP for 48 hours before experiments were performed. All titration experiments were performed as follows: 200 μM of the BRPF1 bromodomain protein was injected into the sample cell using a loading syringe, with 5 mM of histone peptide loaded into the injection syringe. The sample cell received one preliminary injection of 0.5 μL of the histone peptide followed by 19 injections of 2 μL histone peptide. For all titration experiments, each injection was spaced at 150 s time intervals after an initial delay of 60 s, and the injection syringe was stirred continuously at 1000 RPM. The preliminary injection was excluded prior to integration of the binding curve and calculation of the dissociation constants (K_Ds). First, the raw data were corrected for non-specific heats of dilution determined by the magnitude of the peaks appearing after the system reaches complete saturation and normalized for concentration. The raw data were then integrated using a Marquandt nonlinear least-squares analysis according to a 1:1 binding model, normalized for concentration, and analyzed assuming a single set of identical binding sites to calculate the binding affinity, stoichiometry (N), and the thermodynamic values. Binding data for all experiments were analyzed using the ORIGIN 7.0 software (OriginLab Corporation). All experiments where binding occurred were performed in triplicates, while nonbinding experiments were performed in duplicates and standard errors were reported as standard deviations.

bioRxiv preprint doi: https://doi.org/10.1101/2020.02.13.948091; this version posted February 13, 2020. The copyright holder for this preprint (which was not certified by peer review) is the author/funder, who has granted bioRxiv a license to display the preprint in perpetuity. It is made available under aCC-BY-ND 4.0 International license.

Circular dichroism spectroscopy

Circular Dichroism (CD) spectra were recorded on a JASCO J-815 CD Spectrometer (JASCO, Japan) at 25°C in a 1.6 cm cell. BRPF1 bromodomain WT and mutant proteins were dialyzed in CD buffer containing 50 mM NaH_2PO_4 pH 7.0 and 50 mM NaCl and then diluted to between 0.1 μM and 0.5 μM concentration. CD spectra were measured from 199 nm to 260 nm. Two spectra were measured and averaged for each WT and mutant bromodomain protein sample. The spectra were analyzed using the K2D3 structure prediction software [65 66] to determine the percent α-helical and β-sheet content for the WT and each of the mutant BRPF1 bromodomain proteins.

NMR spectroscopy

Chemical shift perturbation experiments were performed using 0.4 mM of uniformly ^{15}N-labeled BRPF1 bromodomain in NMR buffer containing 20 mM Tris-HCl pH 6.8, 150 mM NaCl, 10 mM DTT and 10% D_2O. Titration mixtures of the BRPF1 bromodomain protein and each of the modified histone peptides (H4K5acK8ac residues 1-10, H4K5acK12ac (1-15), H4K5ac (1-10) or 1-15 and H4K8ac (1-10)) were prepared at concentration ratios of 1:0, 1:0.6, 1:1.2, 1:3 and 1:6 in a volume of 150 μL. The sample mixtures were then transferred into 1.7-mm NMR tubes (Bruker). Two-dimensional ^{15}N HSQC (heteronuclear single quantum coherence) experiments for all samples were run at 25°C and NMR data collected as described previously [31]. Normalized chemical shift changes were calculated as described in [67] using the equation:

$$\Delta\delta = \sqrt{{\Delta\delta_H}^2 + (\alpha \cdot \Delta\delta_N)^2}$$

where α = 0.14 for all residues except glycine, which has α = 0.2, and $\Delta\delta_H$ and $\Delta\delta_N$, respectively, are the changes in proton and nitrogen chemical shift in ppm. To map the chemical shift perturbations onto the BRPF1 bromodomain surface, we calculated the standard deviation (σ) of the Euclidean chemical shift change over all residues of all bromodomain:peptide combinations.

bioRxiv preprint doi: https://doi.org/10.1101/2020.02.13.948091; this version posted February 13, 2020. The copyright holder for this preprint (which was not certified by peer review) is the author/funder, who has granted bioRxiv a license to display the preprint in perpetuity. It is made available under aCC-BY-ND 4.0 International license.

Residues whose chemical shift change was greater than 0.5σ were colored yellow, while residues with chemical shift changes greater than 1σ and 2σ were colored orange and red, respectively. The backbone resonance assignments for the BRPF1 bromodomain were completed as previously as described in [31].

Analytical ultracentrifugation

For all AUC experiments, samples of the WT and mutant BRPF1 bromodomain proteins were prepared at an OD_{280} of 0.6 (80.5 μM) in AUC buffer containing 50 mM NaH_2PO_4 pH 7.0, 50 mM NaCl and 1 mM TCEP. The BRPF1 bromodomain protein alone, and in combination with unmodified histone H4 peptide residues 1-15 mixed in a 1:1 molar ratio, were included as controls. All other acetylated histone peptides (H4K5ac 1-15, H4K12ac 1-15, H4K8ac 1-10, H4K5acK8ac 1-10 and H4K5acK12ac 1-15) tested with the BRPF1 bromodomain were also mixed in a 1:1 ratio. AUC measurements were performed at 20°C by UV intensity detection in a Beckman Optima AUC analytical ultracentrifuge at the Center for Analytical Ultracentrifugation of Macromolecular Assemblies at the University of Texas Health Science Center at San Antonio (or at the University of Lethbridge, Alberta, Canada), using an An50Ti rotor and standard 2-channel epon centerpieces (Beckman-Coulter). All the samples were measured in the same run and at multiple wavelengths (278 nm, 280 nm and 282 nm), and the concentrations measured were reported in 280 nm absorbance units. All the AUC data were analyzed with UltraScan-III ver. 4.0, release 2480 [68]. Hydrodynamic corrections for buffer density and viscosity were estimated by UltraScan to be 1.006 g/mL and 1.0239 cP. The partial specific volume of the BRPF1 bromodomain was estimated by UltraScan from protein sequence analogous to methods outlined in Laue et al. Sedimentation Velocity (SV) data were analyzed according to the method described in [69]. Optimization was performed by 2-dimensional spectrum analysis (2DSA) [70] with

bioRxiv preprint doi: https://doi.org/10.1101/2020.02.13.948091; this version posted February 13, 2020. The copyright holder for this preprint (which was not certified by peer review) is the author/funder, who has granted bioRxiv a license to display the preprint in perpetuity. It is made available under aCC-BY-ND 4.0 International license.

simultaneous removal of time- and radially-invariant noise contributions [71]. After inspection of the 2DSA solutions, the fits were further refined using the parametrically constrained spectrum analysis (PCSA) [72], coupled with Monte Carlo analysis to measure confidence limits for the determined parameters [73]. The calculations are computationally intensive and were carried out on high performance computing platforms [74]. All calculations were performed on the Lonestar cluster at the Texas Advanced Computing Center (TACC) at the University of Texas at Austin or on XSEDE clusters at TACC or at the San Diego Supercomputing Center.

AUTHOR INFORMATION

Corresponding Author

*Correspondence to be addressed to Karen C. Glass, Department of Pharmaceutical Sciences, Albany College of Pharmacy and Health Sciences, 261 Mountain View Dr., Colchester, VT 05446, USA.

Email address: karen.glass@acphs.edu

Present Addresses

†If an author's address is different than the one given in the affiliation line, this information may be included here.

Author Contributions

The manuscript was written through contributions of all authors. All authors have given approval to the final version of the manuscript.

bioRxiv preprint doi: https://doi.org/10.1101/2020.02.13.948091; this version posted February 13, 2020. The copyright holder for this preprint (which was not certified by peer review) is the author/funder, who has granted bioRxiv a license to display the preprint in perpetuity. It is made available under aCC-BY-ND 4.0 International license.

Funding Sources

This study was supported by the National Institutes of Health, National Institute of General Medical Sciences award number R15GM104865 to KCG. JO was the recipient of an ACPHS graduate research assistantship from 2018-2019. This study made use of the National Magnetic Resonance Facility at Madison, which is supported by NIH grant P41GM103399. NMRFAM equipment was purchased with funds from the University of Wisconsin-Madison, the NIH P41GM103399, S10RR02781, S10RR08438, S10RR023438, S10RR025062, S10RR029220), the NSF (DMB-8415048, OIA-9977486, BIR-9214394), and the USDA.

Notes

ORCID: Karen C. Glass https://orcid.org/0000-0002-2761-733X

ACKNOWLEDGMENTS

We are thankful to Dr. X.J. Yang at McGill University for providing us with the isolated cDNA from human BRPF1 (Gene ID:7862). This study was supported by the National Institutes of Health, National Institute of General Medical Sciences award number R15GM104865 to KCG. JO was the recipient of an ACPHS graduate research assistantship from 2018-2019. This study made use of the National Magnetic Resonance Facility at Madison, which is supported by NIH grant P41GM103399 (NIGMS), old number: P41RR002301. NMRFAM Equipment was purchased with funds from the University of Wisconsin-Madison, the NIH P41GM103399, S10RR02781, S10RR08438, S10RR023438, S10RR025062, S10RR029220), the NSF (DMB-8415048, OIA-9977486, BIR-9214394), and the USDA. BD acknowledges support from NIH grant GM120600 and NSF grant NSF-ACI-1339649 supporting the development of the UltraScan software. Supercomputer calculations were performed on Comet at the San Diego

bioRxiv preprint doi: https://doi.org/10.1101/2020.02.13.948091; this version posted February 13, 2020. The copyright holder for this preprint (which was not certified by peer review) is the author/funder, who has granted bioRxiv a license to display the preprint in perpetuity. It is made available under aCC-BY-ND 4.0 International license.

Supercomputing Center (support through NSF/XSEDE grant TG-MCB070039N to BD) and on Lonestar-5 at the Texas Advanced Computing Center (supported through UT grant TG457201 to BD).

ABBREVIATIONS

AML, acute myeloid leukemia; AUC, analytical ultracentrifugation; BRPF1, bromodomain-PHD finger protein 1; CD, circular dichroism; DTT, dithiothreitol;HAT, histone acetyltransferase; MEAF6, MYST/Esa1-associated factor 6; ING5, inhibitor of growth 5; ITC, isothermal titration calorimetry; MOZ, monocytic leukemic zinc-finger; NMR, nuclear magnetic resonance; PCR, polymerase chain reaction; PHD, plant homeodomain; PTMs, post-translational modifications; PWWP, proline-tryptophan-tryptophan-proline; SV, sedimentation velocity; TCEP, tris(2-carboxyethyl)phosphine).

bioRxiv preprint doi: https://doi.org/10.1101/2020.02.13.948091; this version posted February 13, 2020. The copyright holder for this preprint (which was not certified by peer review) is the author/funder, who has granted bioRxiv a license to display the preprint in perpetuity. It is made available under aCC-BY-ND 4.0 International license.

REFERENCES

1. Sanchez, R., Meslamani, J. & Zhou, M. M. (2014). The bromodomain: from epigenome reader to druggable target. *Biochim Biophys Acta* **1839**, 676-85.
2. Galvani, A. & Thiriet, C. (2015). Nucleosome Dancing at the Tempo of Histone Tail Acetylation. *Genes (Basel)* **6**, 607-21.
3. Dhalluin, C., Carlson, J. E., Zeng, L., He, C., Aggarwal, A. K. & Zhou, M. M. (1999). Structure and ligand of a histone acetyltransferase bromodomain. *Nature* **399**, 491-6.
4. Filippakopoulos, P., Picaud, S., Mangos, M., Keates, T., Lambert, J. P., Barsyte-Lovejoy, D., Felletar, I., Volkmer, R., Muller, S., Pawson, T., Gingras, A. C., Arrowsmith, C. H. & Knapp, S. (2012). Histone recognition and large-scale structural analysis of the human bromodomain family. *Cell* **149**, 214-31.
5. Arrowsmith, C. H., Bountra, C., Fish, P. V., Lee, K. & Schapira, M. (2012). Epigenetic protein families: a new frontier for drug discovery. *Nat Rev Drug Discov* **11**, 384-400.
6. Hibiya, K., Katsumoto, T., Kondo, T., Kitabayashi, I. & Kudo, A. (2009). Brpf1, a subunit of the MOZ histone acetyl transferase complex, maintains expression of anterior and posterior Hox genes for proper patterning of craniofacial and caudal skeletons. *Dev Biol* **329**, 176-90.
7. Yan, K., Rousseau, J., Littlejohn, R. O., Kiss, C., Lehman, A., Rosenfeld, J. A., Stumpel, C. T. R., Stegmann, A. P. A., Robak, L., Scaglia, F., Nguyen, T. T. M., Fu, H., Ajeawung, N. F., Camurri, M. V., Li, L., Gardham, A., Panis, B., Almannai, M., Sacoto, M. J. G., Baskin, B., Ruivenkamp, C., Xia, F., Bi, W., Study, D. D. D., Study, C., Cho, M. T., Potjer, T. P., Santen, G. W. E., Parker, M. J., Canham, N., McKinnon, M., Potocki, L., MacKenzie, J. J., Roeder, E. R., Campeau, P. M. & Yang, X. J. (2017). Mutations in the Chromatin Regulator Gene BRPF1 Cause Syndromic Intellectual Disability and Deficient Histone Acetylation. *Am J Hum Genet* **100**, 91-104.
8. You, L., Li, L., Zou, J., Yan, K., Belle, J., Nijnik, A., Wang, E. & Yang, X. J. (2016). BRPF1 is essential for development of fetal hematopoietic stem cells. *J Clin Invest* **126**, 3247-62.
9. Laue, K., Daujat, S., Crump, J. G., Plaster, N., Roehl, H. H., Kimmel, C. B., Schneider, R. & Hammerschmidt, M. (2008). The multidomain protein Brpf1 binds histones and is required for Hox gene expression and segmental identity. *Development* **135**, 1935-46.
10. Ullah, M., Pelletier, N., Xiao, L., Zhao, S. P., Wang, K., Degerny, C., Tahmasebi, S., Cayrou, C., Doyon, Y., Goh, S. L., Champagne, N., Cote, J. & Yang, X. J. (2008). Molecular architecture of quartet MOZ/MORF histone acetyltransferase complexes. *Mol Cell Biol* **28**, 6828-43.
11. You, L., Yan, K., Zou, J., Zhao, H., Bertos, N. R., Park, M., Wang, E. & Yang, X. J. (2015). The chromatin regulator Brpf1 regulates embryo development and cell proliferation. *J Biol Chem* **290**, 11349-64.
12. Meier, J. C., Tallant, C., Fedorov, O., Witwicka, H., Hwang, S. Y., van Stiphout, R. G., Lambert, J. P., Rogers, C., Yapp, C., Gerstenberger, B. S., Fedele, V., Savitsky, P., Heidenreich, D., Daniels, D. L., Owen, D. R., Fish, P. V., Igoe, N. M., Bayle, E. D., Haendler, B., Oppermann, U. C. T., Buffa, F., Brennan, P. E., Muller, S., Gingras, A. C., Odgren, P. R., Birnbaum, M. J. & Knapp, S. (2017). Selective Targeting of Bromodomains of the Bromodomain-PHD Fingers Family Impairs Osteoclast Differentiation. *ACS Chem Biol* **12**, 2619-2630.

bioRxiv preprint doi: https://doi.org/10.1101/2020.02.13.948091; this version posted February 13, 2020. The copyright holder for this preprint (which was not certified by peer review) is the author/funder, who has granted bioRxiv a license to display the preprint in perpetuity. It is made available under aCC-BY-ND 4.0 International license.

13. Carlson, S. & Glass, K. C. (2014). The MOZ histone acetyltransferase in epigenetic signaling and disease. *J Cell Physiol* **229**, 1571-4.
14. Li, B., Carey, M. & Workman, J. L. (2007). The role of chromatin during transcription. *Cell* **128**, 707-19.
15. Yun, M., Wu, J., Workman, J. L. & Li, B. (2011). Readers of histone modifications. *Cell Res* **21**, 564-78.
16. Berger, S. L. (2007). The complex language of chromatin regulation during transcription. *Nature* **447**, 407-12.
17. Vermeulen, M., Eberl, H. C., Matarese, F., Marks, H., Denissov, S., Butter, F., Lee, K. K., Olsen, J. V., Hyman, A. A., Stunnenberg, H. G. & Mann, M. (2010). Quantitative interaction proteomics and genome-wide profiling of epigenetic histone marks and their readers. *Cell* **142**, 967-80.
18. Workman, J. L. & Kingston, R. E. (1998). Alteration of nucleosome structure as a mechanism of transcriptional regulation. *Annu Rev Biochem* **67**, 545-79.
19. Flynn, E. M., Huang, O. W., Poy, F., Oppikofer, M., Bellon, S. F., Tang, Y. & Cochran, A. G. (2015). A Subset of Human Bromodomains Recognizes Butyryllysine and Crotonyllysine Histone Peptide Modifications. *Structure* **23**, 1801-14.
20. Dyson, M. H., Rose, S. & Mahadevan, L. C. (2001). Acetyllysine-binding and function of bromodomain-containing proteins in chromatin. *Front Biosci* **6**, D853-65.
21. Borrow, J., Stanton, V. P., Jr., Andresen, J. M., Becher, R., Behm, F. G., Chaganti, R. S., Civin, C. I., Disteche, C., Dube, I., Frischauf, A. M., Horsman, D., Mitelman, F., Volinia, S., Watmore, A. E. & Housman, D. E. (1996). The translocation t(8;16)(p11;p13) of acute myeloid leukaemia fuses a putative acetyltransferase to the CREB-binding protein. *Nat Genet* **14**, 33-41.
22. Dulak, A. M., Stojanov, P., Peng, S., Lawrence, M. S., Fox, C., Stewart, C., Bandla, S., Imamura, Y., Schumacher, S. E., Shefler, E., McKenna, A., Carter, S. L., Cibulskis, K., Sivachenko, A., Saksena, G., Voet, D., Ramos, A. H., Auclair, D., Thompson, K., Sougnez, C., Onofrio, R. C., Guiducci, C., Beroukhim, R., Zhou, Z., Lin, L., Lin, J., Reddy, R., Chang, A., Landrenau, R., Pennathur, A., Ogino, S., Luketich, J. D., Golub, T. R., Gabriel, S. B., Lander, E. S., Beer, D. G., Godfrey, T. E., Getz, G. & Bass, A. J. (2013). Exome and whole-genome sequencing of esophageal adenocarcinoma identifies recurrent driver events and mutational complexity. *Nat Genet* **45**, 478-86.
23. Moore, S. D., Herrick, S. R., Ince, T. A., Kleinman, M. S., Dal Cin, P., Morton, C. C. & Quade, B. J. (2004). Uterine leiomyomata with t(10;17) disrupt the histone acetyltransferase MORF. *Cancer Res* **64**, 5570-7.
24. Panagopoulos, I., Gorunova, L., Bjerkehagen, B. & Heim, S. (2015). Novel KAT6B-KANSL1 fusion gene identified by RNA sequencing in retroperitoneal leiomyoma with t(10;17)(q22;q21). *PLoS One* **10**, e0117010.
25. Lynch, H., Wen, H., Kim, Y. C., Snyder, C., Kinarsky, Y., Chen, P. X., Xiao, F., Goldgar, D., Cowan, K. H. & Wang, S. M. (2013). Can unknown predisposition in familial breast cancer be family-specific? *Breast J* **19**, 520-8.
26. Grasso, C. S., Wu, Y. M., Robinson, D. R., Cao, X., Dhanasekaran, S. M., Khan, A. P., Quist, M. J., Jing, X., Lonigro, R. J., Brenner, J. C., Asangani, I. A., Ateeq, B., Chun, S. Y., Siddiqui, J., Sam, L., Anstett, M., Mehra, R., Prensner, J. R., Palanisamy, N., Ryslik, G. A., Vandin, F., Raphael, B. J., Kunju, L. P., Rhodes, D. R., Pienta, K. J., Chinnaiyan,

bioRxiv preprint doi: https://doi.org/10.1101/2020.02.13.948091; this version posted February 13, 2020. The copyright holder for this preprint (which was not certified by peer review) is the author/funder, who has granted bioRxiv a license to display the preprint in perpetuity. It is made available under aCC-BY-ND 4.0 International license.

A. M. & Tomlins, S. A. (2012). The mutational landscape of lethal castration-resistant prostate cancer. *Nature* **487**, 239-43.

27. Bamborough, P., Barnett, H. A., Becher, I., Bird, M. J., Chung, C. W., Craggs, P. D., Demont, E. H., Diallo, H., Fallon, D. J., Gordon, L. J., Grandi, P., Hobbs, C. I., Hooper-Greenhill, E., Jones, E. J., Law, R. P., Le Gall, A., Lugo, D., Michon, A. M., Mitchell, D. J., Prinjha, R. K., Sheppard, R. J., Watson, A. J. & Watson, R. J. (2016). GSK6853, a Chemical Probe for Inhibition of the BRPF1 Bromodomain. *ACS Med Chem Lett* **7**, 552-7.
28. Bouche, L., Christ, C. D., Siegel, S., Fernandez-Montalvan, A. E., Holton, S. J., Fedorov, O., Ter Laak, A., Sugawara, T., Stockigt, D., Tallant, C., Bennett, J., Monteiro, O., Diaz-Saez, L., Siejka, P., Meier, J., Putter, V., Weiske, J., Muller, S., Huber, K. V. M., Hartung, I. V. & Haendler, B. (2017). Benzoisoquinolinediones as Potent and Selective Inhibitors of BRPF2 and TAF1/TAF1L Bromodomains. *J Med Chem* **60**, 4002-4022.
29. Fernandez-Montalvan, A. E., Berger, M., Kuropka, B., Koo, S. J., Badock, V., Weiske, J., Puetter, V., Holton, S. J., Stockigt, D., Ter Laak, A., Centrella, P. A., Clark, M. A., Dumelin, C. E., Sigel, E. A., Soutter, H. H., Troast, D. M., Zhang, Y., Cuozzo, J. W., Keefe, A. D., Roche, D., Rodeschini, V., Chaikuad, A., Diaz-Saez, L., Bennett, J. M., Fedorov, O., Huber, K. V. M., Hubner, J., Weinmann, H., Hartung, I. V. & Gorjanacz, M. (2017). Isoform-Selective ATAD2 Chemical Probe with Novel Chemical Structure and Unusual Mode of Action. *ACS Chem Biol*.
30. Clark, P. G., Vieira, L. C., Tallant, C., Fedorov, O., Singleton, D. C., Rogers, C. M., Monteiro, O. P., Bennett, J. M., Baronio, R., Muller, S., Daniels, D. L., Mendez, J., Knapp, S., Brennan, P. E. & Dixon, D. J. (2015). LP99: Discovery and Synthesis of the First Selective BRD7/9 Bromodomain Inhibitor. *Angew Chem Int Ed Engl* **54**, 6217-21.
31. Poplawski, A., Hu, K., Lee, W., Natesan, S., Peng, D., Carlson, S., Shi, X., Balaz, S., Markley, J. L. & Glass, K. C. (2014). Molecular insights into the recognition of N-terminal histone modifications by the BRPF1 bromodomain. *J Mol Biol* **426**, 1661-76.
32. Huang, H., Sabari, B. R., Garcia, B. A., Allis, C. D. & Zhao, Y. (2014). SnapShot: histone modifications. *Cell* **159**, 458-458 e1.
33. Young, N. L., DiMaggio, P. A., Plazas-Mayorca, M. D., Baliban, R. C., Floudas, C. A. & Garcia, B. A. (2009). High throughput characterization of combinatorial histone codes. *Mol Cell Proteomics* **8**, 2266-84.
34. Wang, T., Holt, M. V. & Young, N. L. (2018). The histone H4 proteoform dynamics in response to SUV4-20 inhibition reveals single molecule mechanisms of inhibitor resistance. *Epigenetics Chromatin* **11**, 29.
35. Jiang, T., Hoover, M. E., Holt, M. V., Freitas, M. A., Marshall, A. G. & Young, N. L. (2018). Middle-Down Characterization of the Cell Cycle Dependence of Histone H4 Posttranslational Modifications and Proteoforms. *Proteomics* **18**, e1700442.
36. Moriniere, J., Rousseaux, S., Steuerwald, U., Soler-Lopez, M., Curtet, S., Vitte, A. L., Govin, J., Gaucher, J., Sadoul, K., Hart, D. J., Krijgsveld, J., Khochbin, S., Muller, C. W. & Petosa, C. (2009). Cooperative binding of two acetylation marks on a histone tail by a single bromodomain. *Nature* **461**, 664-8.
37. Koo, S. J., Fernandez-Montalvan, A. E., Badock, V., Ott, C. J., Holton, S. J., von Ahsen, O., Toedling, J., Vittori, S., Bradner, J. E. & Gorjanacz, M. (2016). ATAD2 is an epigenetic reader of newly synthesized histone marks during DNA replication. *Oncotarget* **7**, 70323-70335.

bioRxiv preprint doi: https://doi.org/10.1101/2020.02.13.948091; this version posted February 13, 2020. The copyright holder for this preprint (which was not certified by peer review) is the author/funder, who has granted bioRxiv a license to display the preprint in perpetuity. It is made available under aCC-BY-ND 4.0 International license.

38. Tallant, C., Valentini, E., Fedorov, O., Overvoorde, L., Ferguson, F. M., Filippakopoulos, P., Svergun, D. I., Knapp, S. & Ciulli, A. (2015). Molecular basis of histone tail recognition by human TIP5 PHD finger and bromodomain of the chromatin remodeling complex NoRC. *Structure* **23**, 80-92.
39. Poncet-Montange, G., Zhan, Y., Bardenhagen, J. P., Petrocchi, A., Leo, E., Shi, X., Lee, G. R. t., Leonard, P. G., Geck Do, M. K., Cardozo, M. G., Andersen, J. N., Palmer, W. S., Jones, P. & Ladbury, J. E. (2015). Observed bromodomain flexibility reveals histone peptide- and small molecule ligand-compatible forms of ATAD2. *Biochem J* **466**, 337-46.
40. Zhu, J. & Caflisch, A. (2016). Twenty Crystal Structures of Bromodomain and PHD Finger Containing Protein 1 (BRPF1)/Ligand Complexes Reveal Conserved Binding Motifs and Rare Interactions. *J Med Chem* **59**, 5555-61.
41. Langini, C., Caflisch, A. & Vitalis, A. (2017). The ATAD2 bromodomain binds different acetylation marks on the histone H4 in similar fuzzy complexes. *J Biol Chem* **292**, 16734-16745.
42. Lubula, M. Y., Eckenroth, B. E., Carlson, S., Poplawski, A., Chruszcz, M. & Glass, K. C. (2014). Structural insights into recognition of acetylated histone ligands by the BRPF1 bromodomain. *FEBS Lett* **588**, 3844-54.
43. Ferri, E., Petosa, C. & McKenna, C. E. (2016). Bromodomains: Structure, function and pharmacology of inhibition. *Biochem Pharmacol* **106**, 1-18.
44. Ladurner, A. G., Inouye, C., Jain, R. & Tjian, R. (2003). Bromodomains mediate an acetyl-histone encoded antisilencing function at heterochromatin boundaries. *Mol Cell* **11**, 365-76.
45. Kanno, T., Kanno, Y., Siegel, R. M., Jang, M. K., Lenardo, M. J. & Ozato, K. (2004). Selective recognition of acetylated histones by bromodomain proteins visualized in living cells. *Mol Cell* **13**, 33-43.
46. Gay, J. C., Eckenroth, B. E., Evans, C. M., Langini, C., Carlson, S., Lloyd, J. T., Caflisch, A. & Glass, K. C. (2019). Disulfide bridge formation influences ligand recognition by the ATAD2 bromodomain. *Proteins* **87**, 157-167.
47. Zhu, J., Zhou, C. & Caflisch, A. (2018). Structure-based discovery of selective BRPF1 bromodomain inhibitors. *European Journal of Medicinal Chemistry*.
48. Du, X., Li, Y., Xia, Y. L., Ai, S. M., Liang, J., Sang, P., Ji, X. L. & Liu, S. Q. (2016). Insights into Protein-Ligand Interactions: Mechanisms, Models, and Methods. *Int J Mol Sci* **17**.
49. Dunitz, J. D. (1995). Win some, lose some: enthalpy-entropy compensation in weak intermolecular interactions. *Chem Biol* **2**, 709-12.
50. Leroy, G., Dimaggio, P. A., Chan, E. Y., Zee, B. M., Blanco, M. A., Bryant, B., Flaniken, I. Z., Liu, S., Kang, Y., Trojer, P. & Garcia, B. A. (2013). A quantitative atlas of histone modification signatures from human cancer cells. *Epigenetics Chromatin* **6**, 20.
51. Shang, E., Nickerson, H. D., Wen, D., Wang, X. & Wolgemuth, D. J. (2007). The first bromodomain of Brdt, a testis-specific member of the BET sub-family of double-bromodomain-containing proteins, is essential for male germ cell differentiation. *Development* **134**, 3507-15.
52. Zhang, Y. & Reinberg, D. (2001). Transcription regulation by histone methylation: interplay between different covalent modifications of the core histone tails. *Genes Dev* **15**, 2343-60.

bioRxiv preprint doi: https://doi.org/10.1101/2020.02.13.948091; this version posted February 13, 2020. The copyright holder for this preprint (which was not certified by peer review) is the author/funder, who has granted bioRxiv a license to display the preprint in perpetuity. It is made available under aCC-BY-ND 4.0 International license.

53. Dillon, S. C., Zhang, X., Trievel, R. C. & Cheng, X. (2005). The SET-domain protein superfamily: protein lysine methyltransferases. *Genome Biol* **6**, 227.
54. Murray, K. (1964). The Occurrence of Epsilon-N-Methyl Lysine in Histones. *Biochemistry* **3**, 10-5.
55. Rossetto, D., Avvakumov, N. & Cote, J. (2012). Histone phosphorylation: a chromatin modification involved in diverse nuclear events. *Epigenetics* **7**, 1098-108.
56. Cheung, W. L., Turner, F. B., Krishnamoorthy, T., Wolner, B., Ahn, S. H., Foley, M., Dorsey, J. A., Peterson, C. L., Berger, S. L. & Allis, C. D. (2005). Phosphorylation of histone H4 serine 1 during DNA damage requires casein kinase II in S. cerevisiae. *Curr Biol* **15**, 656-60.
57. Sun, H., Liu, J., Zhang, J., Shen, W., Huang, H., Xu, C., Dai, H., Wu, J. & Shi, Y. (2007). Solution structure of BRD7 bromodomain and its interaction with acetylated peptides from histone H3 and H4. *Biochem Biophys Res Commun* **358**, 435-41.
58. Krissinel, E. (2007). On the relationship between sequence and structure similarities in proteomics. *Bioinformatics* **23**, 717-23.
59. Romero, F. A., Taylor, A. M., Crawford, T. D., Tsui, V., Cote, A. & Magnuson, S. (2016). Disrupting Acetyl-Lysine Recognition: Progress in the Development of Bromodomain Inhibitors. *J Med Chem* **59**, 1271-98.
60. Crawford, T. D., Tsui, V., Flynn, E. M., Wang, S. M., Taylor, A. M., Cote, A., Audia, J. E., Beresini, M. H., Burdick, D. J., Cummings, R., Dakin, L. A., Duplessis, M., Good, A. C., Hewitt, M. C., Huang, H. R., Jayaram, H., Kiefer, J. R., Jiang, Y., Murray, J., Nasveschuk, C. G., Pardo, E., Poy, F., Romero, F. A., Tang, Y., Wang, J., Xu, Z. W., Zawadzke, L. E., Zhu, X. Y., Albrecht, B. K., Magnuson, S. R., Bellon, S. & Cochran, A. G. (2016). Diving into the Water: Inducible Binding Conformations for BRD4, TAF1(2), BRD9, and CECR2 Bromodomains. *Journal of Medicinal Chemistry* **59**, 5391-5402.
61. Carapeti, M., Aguiar, R. C., Goldman, J. M. & Cross, N. C. (1998). A novel fusion between MOZ and the nuclear receptor coactivator TIF2 in acute myeloid leukemia. *Blood* **91**, 3127-33.
62. Crowley, J. A., Wang, Y., Rapoport, A. P. & Ning, Y. (2005). Detection of MOZ-CBP fusion in acute myeloid leukemia with 8;16 translocation. *Leukemia* **19**, 2344-5.
63. Kitabayashi, I., Aikawa, Y., Yokoyama, A., Hosoda, F., Nagai, M., Kakazu, N., Abe, T. & Ohki, M. (2001). Fusion of MOZ and p300 histone acetyltransferases in acute monocytic leukemia with a t(8;22)(p11;q13) chromosome translocation. *Leukemia* **15**, 89-94.
64. Champagne, K. S., Piscitelli, E. & Francklyn, C. S. (2006). Substrate recognition by the hetero-octameric ATP phosphoribosyltransferase from Lactococcus lactis. *Biochemistry* **45**, 14933-43.
65. Louis-Jeune, C., Andrade-Navarro, M. A. & Perez-Iratxeta, C. (2012). Prediction of protein secondary structure from circular dichroism using theoretically derived spectra. *Proteins* **80**, 374-81.
66. Andrade, M. A., Chacon, P., Merelo, J. J. & Moran, F. (1993). Evaluation of secondary structure of proteins from UV circular dichroism spectra using an unsupervised learning neural network. *Protein Eng* **6**, 383-90.
67. Williamson, M. P. (2013). Using chemical shift perturbation to characterise ligand binding. *Prog Nucl Magn Reson Spectrosc* **73**, 1-16.

bioRxiv preprint doi: https://doi.org/10.1101/2020.02.13.948091; this version posted February 13, 2020. The copyright holder for this preprint (which was not certified by peer review) is the author/funder, who has granted bioRxiv a license to display the preprint in perpetuity. It is made available under aCC-BY-ND 4.0 International license.

68. Demeler, B. & Gorbet, G. E. (2016). Analytical Ultracentrifugation Data Analysis with UltraScan-III. In *Analytical Ultracentrifugation: Instrumentation, Software, and Applications* (Uchiyama, S., Arisaka, F., Stafford, W. F. & Laue, T., eds.), pp. 119-143. Springer Japan, Tokyo.
69. Demeler, B. (2010). Methods for the design and analysis of sedimentation velocity and sedimentation equilibrium experiments with proteins. *Curr Protoc Protein Sci* **Chapter 7**, Unit 7 13.
70. Brookes, E., Cao, W. & Demeler, B. (2010). A two-dimensional spectrum analysis for sedimentation velocity experiments of mixtures with heterogeneity in molecular weight and shape. *Eur Biophys J* **39**, 405-14.
71. Schuck, P. & Demeler, B. (1999). Direct sedimentation analysis of interference optical data in analytical ultracentrifugation. *Biophys J* **76**, 2288-96.
72. Gorbet, G., Devlin, T., Hernandez Uribe, B. I., Demeler, A. K., Lindsey, Z. L., Ganji, S., Breton, S., Weise-Cross, L., Lafer, E. M., Brookes, E. H. & Demeler, B. (2014). A parametrically constrained optimization method for fitting sedimentation velocity experiments. *Biophys J* **106**, 1741-50.
73. Demeler, B. & Brookes, E. (2008). Monte Carlo analysis of sedimentation experiments. *Colloid and Polymer Science* **286**, 129-137.
74. Brookes, E. & Demeler, B. (2008). Parallel computational techniques for the analysis of sedimentation velocity experiments in UltraScan. *Colloid and Polymer Science* **286**, 139-148.

bioRxiv preprint doi: https://doi.org/10.1101/2020.02.13.948091; this version posted February 13, 2020. The copyright holder for this preprint (which was not certified by peer review) is the author/funder, who has granted bioRxiv a license to display the preprint in perpetuity. It is made available under aCC-BY-ND 4.0 International license.

Figure 1

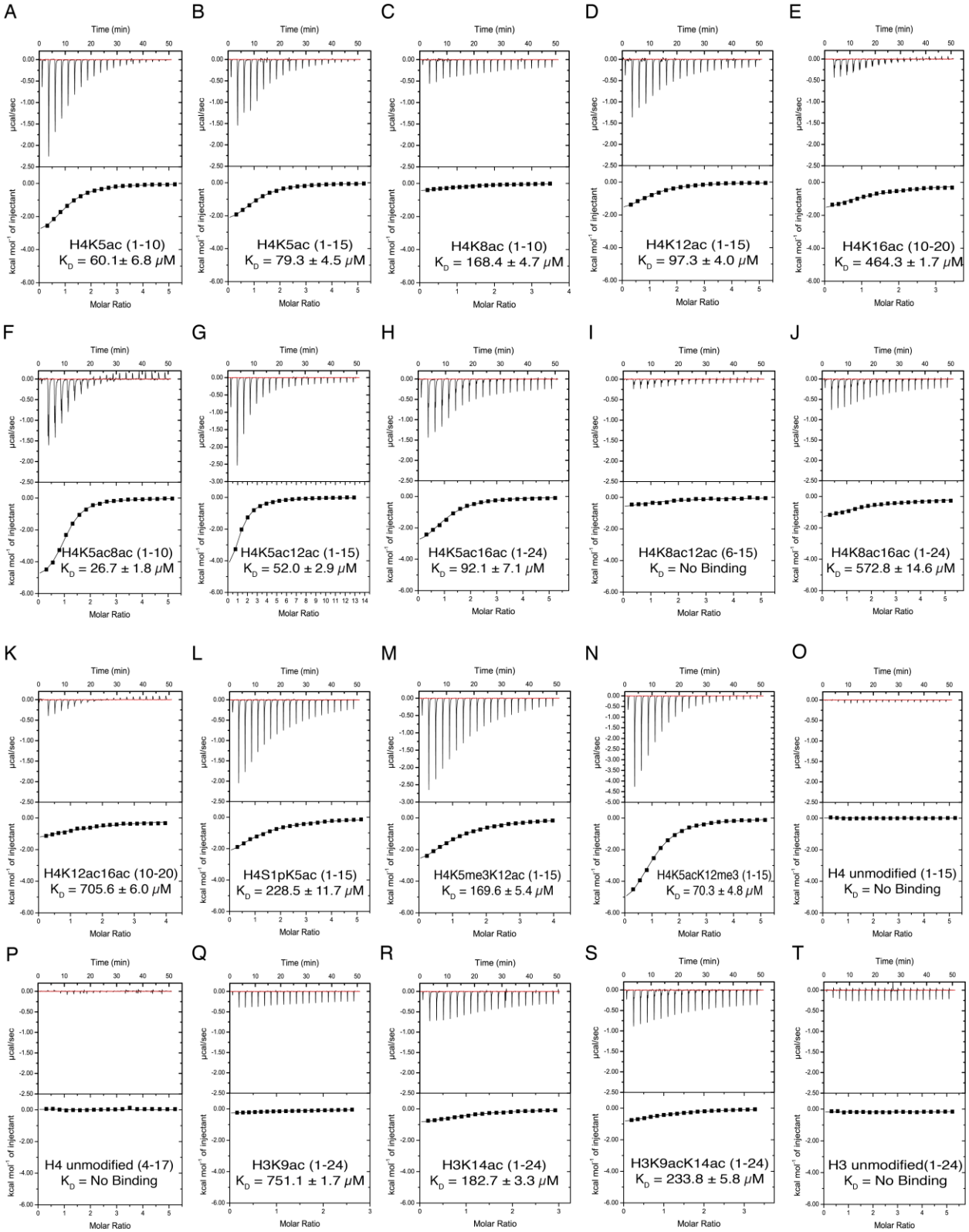

bioRxiv preprint doi: https://doi.org/10.1101/2020.02.13.948091; this version posted February 13, 2020. The copyright holder for this preprint (which was not certified by peer review) is the author/funder, who has granted bioRxiv a license to display the preprint in perpetuity. It is made available under aCC-BY-ND 4.0 International license.

Figure 2

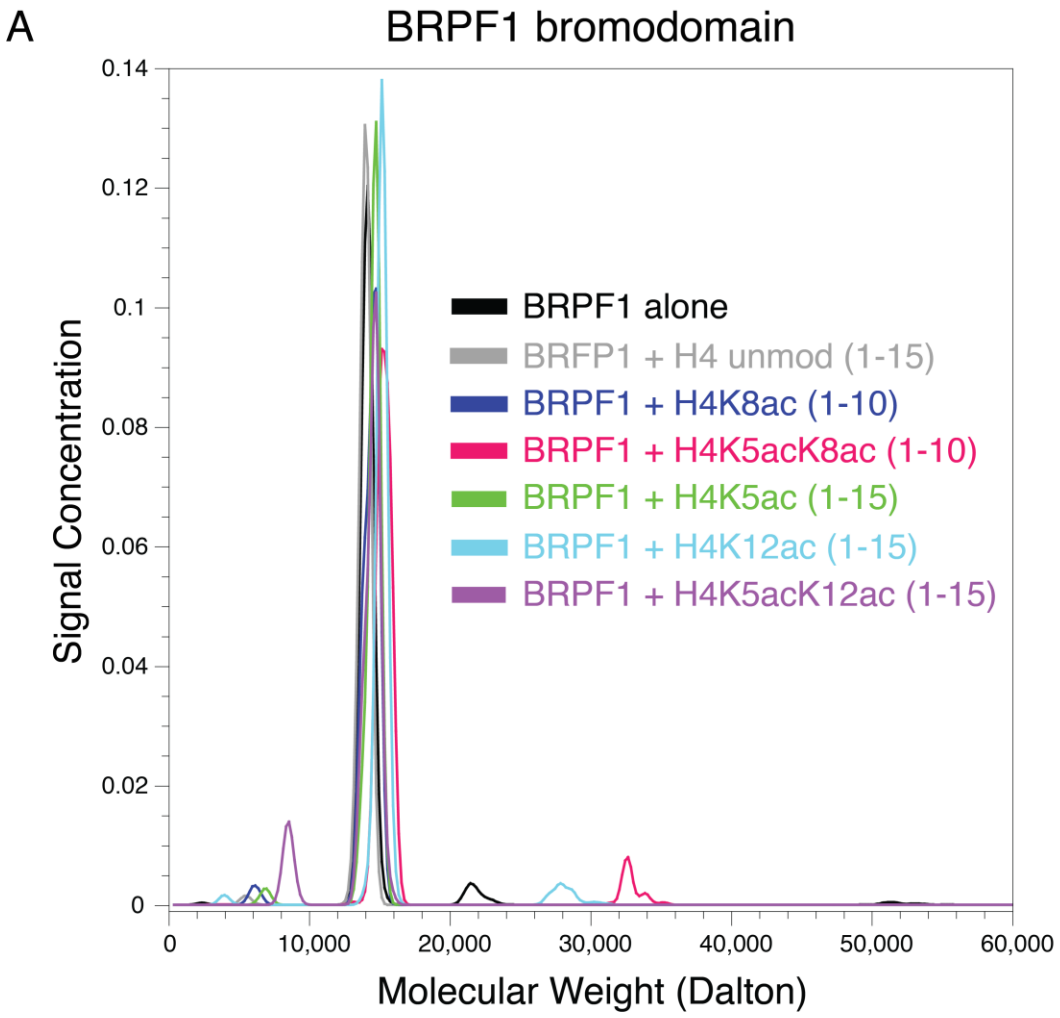

bioRxiv preprint doi: https://doi.org/10.1101/2020.02.13.948091; this version posted February 13, 2020. The copyright holder for this preprint (which was not certified by peer review) is the author/funder, who has granted bioRxiv a license to display the preprint in perpetuity. It is made available under aCC-BY-ND 4.0 International license.

Figure 3

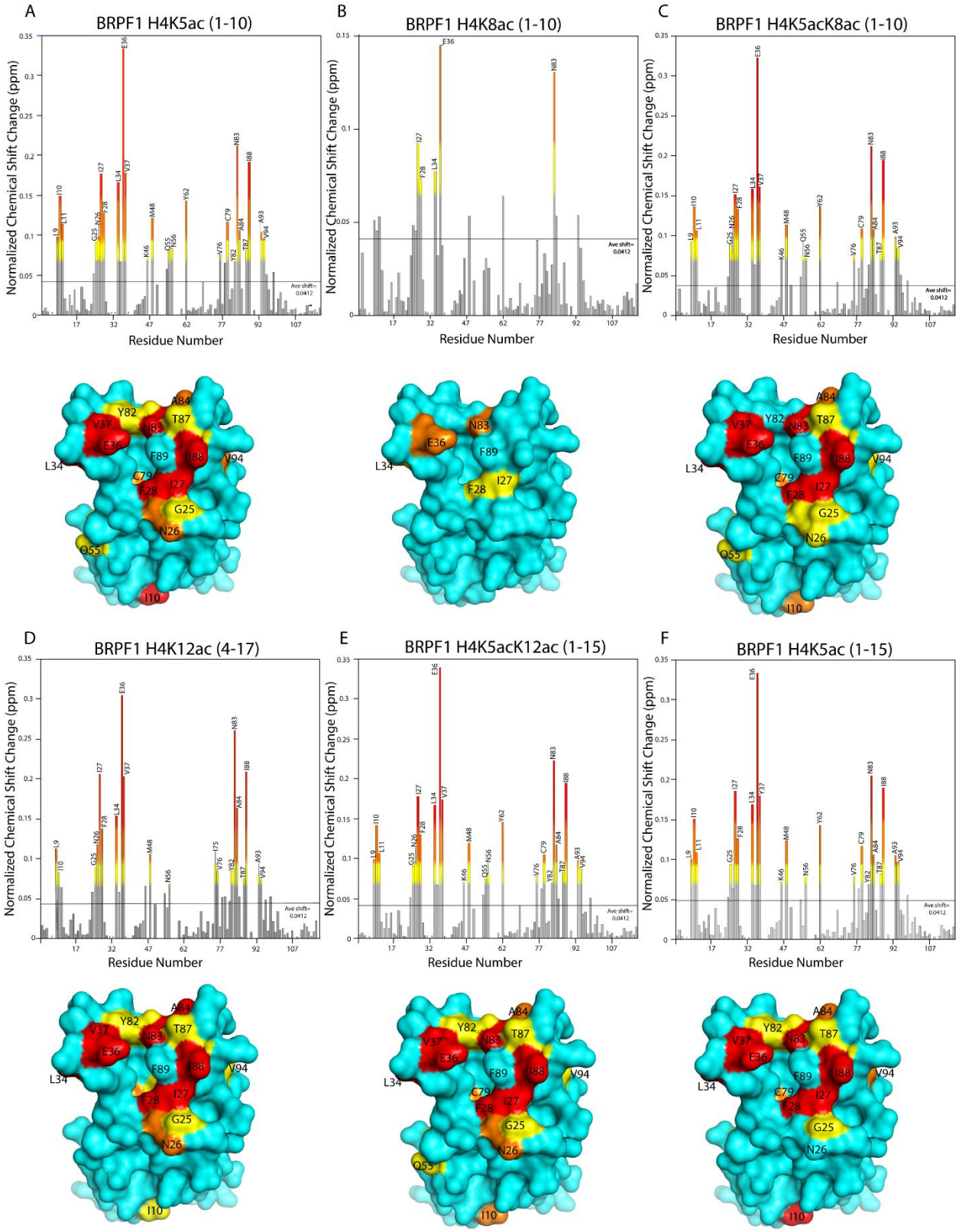

bioRxiv preprint doi: https://doi.org/10.1101/2020.02.13.948091; this version posted February 13, 2020. The copyright holder for this preprint (which was not certified by peer review) is the author/funder, who has granted bioRxiv a license to display the preprint in perpetuity. It is made available under aCC-BY-ND 4.0 International license.

Figure 4

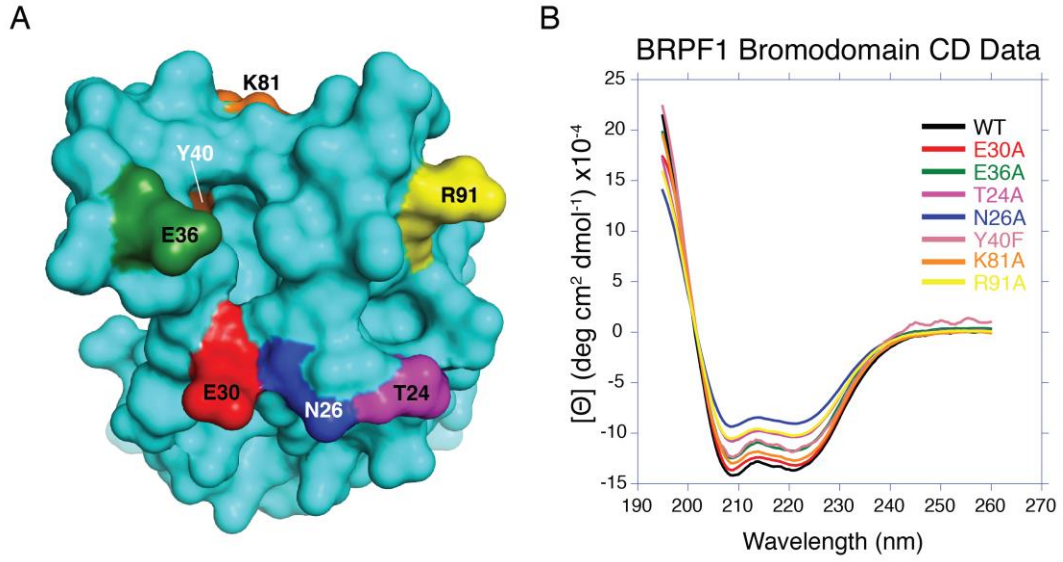

bioRxiv preprint doi: https://doi.org/10.1101/2020.02.13.948091; this version posted February 13, 2020. The copyright holder for this preprint (which was not certified by peer review) is the author/funder, who has granted bioRxiv a license to display the preprint in perpetuity. It is made available under aCC-BY-ND 4.0 International license.

Figure 5

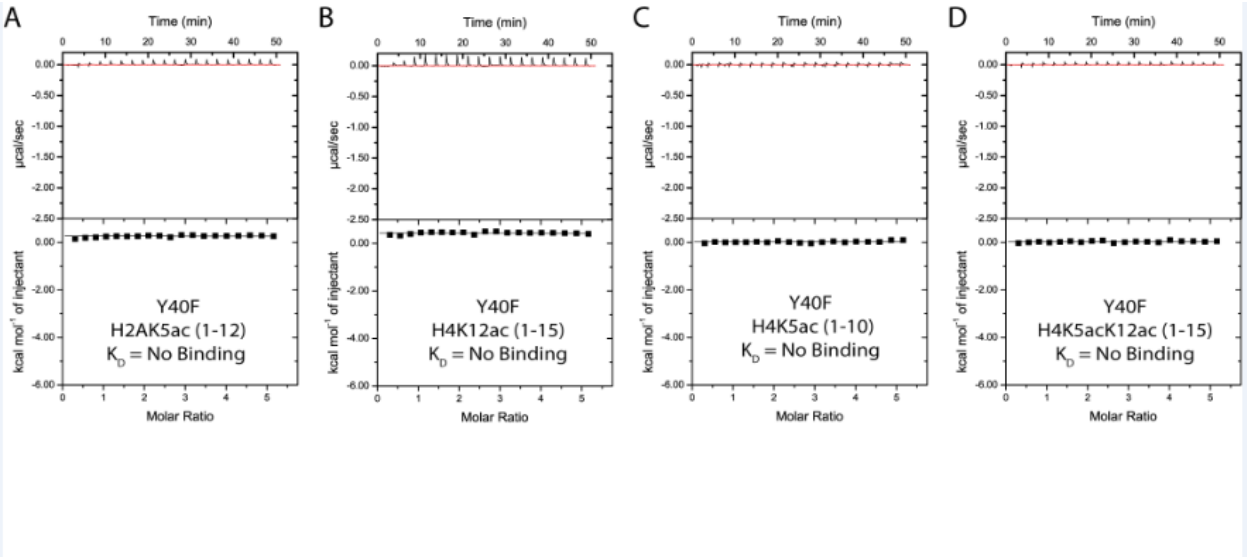

bioRxiv preprint doi: https://doi.org/10.1101/2020.02.13.948091; this version posted February 13, 2020. The copyright holder for this preprint (which was not certified by peer review) is the author/funder, who has granted bioRxiv a license to display the preprint in perpetuity. It is made available under aCC-BY-ND 4.0 International license.

FIGURE LEGENDS:

Figure 1. ITC measurements of the interactions between the BRPF1 bromodomain and acetylated histone ligands. (A-P). Exothermic ITC enthalpy plots for the binding of the BRPF1 bromodomain to mono-, di- and unacetylated histone H4 peptides. The calculated dissociation constants are indicated for each peptide tested.

Figure 2. Molecular weight distributions of the BRPF1 bromodomain alone and in complex with mono- and di-acetylated histone ligands, determined by analytical ultracentrifugation. The distribution shows the molecular weights of the BRPF1 bromodomain alone and a 1:1 combination ratio with H4K5ac (1-15), H4K5acK12ac (1-15), H4K12ac (1-15), H4 unmodified (1-15), H4K5acK8ac (1-10) and H4K8ac (1-10) colored in red, blue, magenta, purple, green, black, and cyan respectively. All molar masses are consistent with a 1:1 ratio of BRPF1 bromodomain and histone peptide.

Figure 3. Mapping of the mono- and di-acetylated histone ligand binding interfaces on the BRPF1 bromodomain.
(A-F). Histograms show the normalized ^{1}H-^{15}N chemical shift changes in the backbone amides of the BRPF1 bromodomain in the presence of H4K5ac (1-10) (A), H4K8ac (1-10) (B), H4K5acK8ac (1-10) (C), H4K12ac (4-17) (D), H4K5acK12ac (1-15) (E), and H4K5ac (1-15) (F). Chemical shift changes 0.5, 1 and 2 standard deviations away from the average shift change are colored yellow, orange and red respectively. Amino acid residues with significant chemical shift perturbations upon addition of the histone ligands are mapped onto the surface of the apo structure of the BRPF1 bromodomain (PDBID: 2D9E).

Figure 4. Circular dichroism spectra of the wild-type and mutant BRPF1 bromodomains. (A). Surface representation of the apo structure (cyan) of the BRPF1 bromodomain showing mutated residues. The amino acid residues N26, T24, E30, E36, Y40, K81 and R91 mutated to alanine are indicated as shown. (B). Secondary structure of the BRPF1 bromodomain wild-type and mutant bromodomain proteins measured by circular dichroism. Circular dichroism molar ellipticity plots of the BRPF1 wild type and mutant bromodomains are shown. Each protein is represented by a different color and all show clear α-helical structure to match the wild type BRPF1 bromodomain.

Figure 5. ITC measurements of the Y40F mutant bromodomain involved in water coordination, with acetylated histone peptides. No binding was detected for all the four histone peptides tested with the Y40F mutant bromodomain which shows its important role in water coordination in the bromodomain binding pocket.

bioRxiv preprint doi: https://doi.org/10.1101/2020.02.13.948091; this version posted February 13, 2020. The copyright holder for this preprint (which was not certified by peer review) is the author/funder, who has granted bioRxiv a license to display the preprint in perpetuity. It is made available under aCC-BY-ND 4.0 International license.

TABLES:

Table 1: Sequences of the mono- and di-acetylated histone peptides studied, and the dissociation constants of their complexes with the BRPF1 bromodomain as measured by ITC.

Histone peptide	Sequence	BRPF1 K_D (μM)	N value	ΔH (cal/Mol)	ΔS (cal/Mol/deg)
H3 unmodified (1-24)	ARTKQTARKSTGGKAPRKQLATKA	No binding	---	---	---
H3K9ac (1-24)	ARTKQTAR(Kac)STGGKAPRKQLATKA	751.1 ± 1.7	1.0 ± 0.0	-965.5 ± 221.4	10.8 ± 0.8
H3K14ac (8-19)[1]	RKSTGG(Kac)APRKQ	626	---	---	---
H3K14ac (1-24)	ARTKQTARKSTGG(Kac)APRKQLATKA	182.7 ± 3.3	1.0 ± 0.0	-961.6 ± 653.7	13.6 ± 2.4
H3K9acK14ac (1-24)	ARTKQTAR(Kac)STGG(Kac)APRKQLATKA	233.8 ± 5.8	1.0 ± 0.0	-1249.3 ± 136.7	12.1 ± 0.5
H4 unmodified (1-15)	SGRGKGGKGLGKGGA	No binding	---	---	---
H4K5ac (1-10)	SGRG(Kac)GGKGL	60.1 ± 6.8	0.9 ± 0.1	-3899.7 ± 347.5	5.3 ± 1.3
H4K5ac (1-15)	SGRG(Kac)GGKGLGKGGA	79.3 ± 4.5	1.0 ± 0.1	-3671.7 ± 925.3	5.6 ± 3.4
H4K5ac (4-17)[1]	G(Kac)GGKGLGKGGAKR	1236*	---	---	---
H4K8ac (1-10)	SGRGKGG(Kac)GL	168.4 ± 4.7	1.1 ± 0.2	-574.6 ± 202.5	15.2 ± 0.8
H4K8ac (4-17)[1]	GKGG(Kac)GLGKGGAKR	697*	---	---	---
H4K12ac (1-15)	SGRGKGGKGLG(Kac)GGA	97.3 ± 4.0	1.0 ± 0.1	-2401.0 ± 598.9	9.7 ± 2.1
H4K12ac (4-17)[1]	GKGGKGLG(Kac)GGAKR	86.5 ± 9.1	---	---	---
H4K16ac (10-20)	LGKGGA(Kac)RHRK	464.3 ± 1.7	1.1 ± 0.1	-3607.3 ± 553.1	2.3 ± 2.0
H4K5acK8ac (1-10)	SGRG(Kac)GG(Kac)GL	26.7 ± 1.8	1.0 ± 0.0	-8023.3 ± 4744.7	-7.9 ± 16.9
H4K5acK12ac (1-15)	SGRG(Kac)GGKGLG(Kac)GGA	52.0 ± 2.9	1.0 ± 0.0	-7395.0 ± 676.0	-7.0 ± 2.4
H4K5acK16ac (1-24)	SGRG(Kac)GGKGLGKGGA(Kac)RHRKVLRD	92.1 ± 7.1	1.0 ± 0.1	-4476.3 ± 534.7	2.4 ± 2.1
H4K8acK12ac (6-15)	GG(Kac)GLG(Kac)GGA	No binding	---	---	---
H4K8acK16ac (1-24)	SGRGKGG(Kac)GLGKGGA(Kac)RHRKVLRD	572.8 ± 14.6	1.0 ± 0.0	-6664.3 ± 5073.6	-9.1 ± 18.3
H4K12acK16ac (10-20)	LG(Kac)GGA(Kac)RHRK	705.6 ± 6.0	1.0 ± 0.0	-5040.3 ± 979.5	-3.7 ± 3.5
H4S1phosK5ac (1-15)	(Sp)GRG(Kac)GGKGLGKGGA	228.5 ± 11.7	1.1 ± 0.1	-3742.7 ± 830.1	3.2 ± 3.1
H4K5me3K12ac (1-15)	SGRG(Kme3)GGKGLG(Kac)GGA	169.6 ± 5.4	1.0 ± 0.0	-4168.7 ± 277.3	2.3 ± 1.0
H4K5acK12me3 (1-15)	SGRG(Kac)GGKGLG(Kme3)GGA	70.3 ± 4.8	1.1 ± 0.0	-6357.0 ± 205.9	-3.8 ± 0.6

[1] Previously published BRPF1 binding data [31]

bioRxiv preprint doi: https://doi.org/10.1101/2020.02.13.948091; this version posted February 13, 2020. The copyright holder for this preprint (which was not certified by peer review) is the author/funder, who has granted bioRxiv a license to display the preprint in perpetuity. It is made available under aCC-BY-ND 4.0 International license.

* Indicates dissociation constants measured by NMR titration experiments.

Table 2. Dissociation constants of the wild-type and mutant BRPF1 bromodomain proteins with histone ligands as measured by ITC experiments.

BRPF1	H4K5ac (1-10), N	H4K12ac (1-15), N	H4K5K8ac (1-10), N	H4K5K12ac (1-15), N
Wild type	60.1 ± 6.8, 0.9 ± 0.1	97.3 ± 4.0, 1.0 ± 0.1	26.7 ± 1.8, 1.0 ± 0.0	52.0 ± 2.9, 1.0 ± 0.0
T24A	28.9 ± 1.0, 1.0 ± 0.0	105.7 ± 8.3, 0.9 ± 0.1	99.4 ± 5.3, 1.0 ± 0.1	31.2 ± 4.6, 1.0 ± 0.0
E30A	79.4 ± 5.7, 1.1 ± 0.1	104.5 ± 4.0, 1.1 ± 0.0	27.2 ± 0.7, 1.0 ± 0.0	39.0 ± 1.6, 1 ± 0.0
E36A	51.4 ± 1.9, 1.0 ± 0.0	54.7 ± 5.5, 1.0 ± 0.0	43.1 ± 1.4, 1 ± 0.0	31.0 ± 2.6, 1.0 ± 0.0
K81A	59.9 ± 3.8, 1.0 ± 0.0	45.0 ± 3.0, 1.0 ± 0.0	45.7 ± 5.6, 1 ± 0.0	24.6 ± 0.8, 1.0 ± 0.0
R91A	37.3 ± 1.3, 1.0 ± 0.0	79.7 ± 5.1, 1.0 ± 0.0	21.5 ± 1.9, 0.9 ± 0.0	23.0 ± 3.8, 1.0 ± 0.0
N26A	44.1 ± 0.9, 1.0 ± 0.0	122.3 ± 2.9, 1.2 ± 0.1	34.5 ± 1.3, 1.0 ± 0.0	34.2 ± 6.8, 1.0 ± 0.0

Table 3: Percentages of α-helix and β-strand composition in wild-type (WT) and mutant BRPF1 bromodomain proteins calculated from circular dichroism experiments.

BRPF1 bromodomain	% alpha helix	% beta strand
WT	93.85%	0.42%
T24A	93.71%	0.44%
E30A	93.69%	0.43%
E36A	93.83%	0.43%
K81A	93.90%	0.41%
R91A	93.71%	0.44%
N26A	93.73%	0.44%
Y40F	42.96%	17.81%